Abstract

When a glass comes in contact with an environment, such as flowing or stagnant groundwater, corrosive gases and vapors, or aqueous solutions, chemical reactions occur at the surface, and then spread to the whole of the glass, depending on its composition, the pH of the solution, and the temperature of the environment. This overview is an attempt to consolidate the understanding that can be obtained on dissolution behavior of glasses designed for the disposal of nuclear waste. Since glass dissolution is not an intrinsic property, the observed behavior depends on the test conditions and test methods. Current understanding of glass dissolution behavior is based on several in-depth studies that have been conducted in the last 30 years. These studies have focused on understanding two aspects of chemical durability of nuclear waste glasses. First, the ability to predict glass durability and produce glasses to meet specific leaching criteria based on short-term tests, and, secondly, the ability to predict the long-term (on the order of 10,000 yr or more) dissolution behavior of glasses. Several attempts have been made to correlate chemical durability and glass composition using thermodynamic, structural, and empirical models. The importance of glass dissolution models in predicting glass performance over extended periods of time is discussed.

Chemical durability of nuclear waste glasses–a review

V. Jain
Center For Nuclear Waste Regulatory Analyses
Southwest Research Institute

INTRODUCTION

When a glass comes in contact with an environment, such as flowing or stagnant groundwater, corrosive gases and vapors, or aqueous solutions, chemical reactions occur at the surface, and then spread to the whole of the glass, depending on its composition, the pH of the solution, and the temperature of the environment. Newton[1] provides an excellent historical review, dating back to 1660, of the chemical durability of glasses. The modern understanding of chemical durability of glasses has developed in the last 30 years. These studies have focused on understanding two aspects of chemical durability of nuclear waste glasses. First, the ability to predict glass durability and produce glasses to meet specific leaching criteria based on short-term tests, and, secondly, the ability to predict the long-term (on the order of 10,000 years or more) dissolution behavior of glasses. In recent years, studies attempt to measure the durability of glasses developed for the disposal of high-level radioactive wastes. Various aspects of the chemical durability of glasses have been reviewed by Paul,[2] Jantzen,[3] Ellison,[4] Bourcier,[5] and the U.S. Department of Energy.[6]

This review provides an overview of the current understanding of glass dissolution behavior in nuclear waste glasses. Since glass corrosion is not an intrinsic property of the materials, the observed dissolution behavior depends on the test conditions and test methods. Several methods have been developed for accelerated testing to determine the corrosion behavior of glasses. A few test methods that form the basis of current understanding are discussed, as well as relationships between glass composition and environment (pH, temperature, and nature of solution). A careful evaluation is required before drawing conclusions regarding

the chemical durability of a glass based solely on data. In this report, the terms glass durability, corrosion of glass, or dissolution of glass are interchangeably used to refer to glass corrosion.

GLASS CORROSION MECHANISM

Glass reactions in aqueous environments are complex and depend on glass composition and contact solution chemistry. The processes involved in glass dissolution include ion-exchange, water diffusion, hydrolysis, and precipitation. Even though dissolution may start by simple ion-exchange or hydrolysis reaction, the simultaneous occurrence of the stated processes is not uncommon. The initial reaction on the glass surface depends on the contact-solution chemistry. In contact with water at neutral pH, the dissolution behavior of a simple alkali silicate glass is controlled by the hydrolysis reaction expressed by equation (1). Alkaline pH involves network hydrolysis of Si-O-Si bonds, as shown by equation (2) and (3). In acidic pH, the reaction begins with an ion-exchange reaction between alkali ions (M^+ ions) in the glass and the hydrogen ions (hydronium ions, H_3O^+) in the solution, as shown by equation (4). In 1980, Ernsberger[7] pointed out that the field intensity of the bare proton is so high that it cannot exist in a condensed phase, and the proton is probably associated with water molecules (H_3O^+). The interrelationship between reactions was described by Paul.[8] He stated that, in neutral solutions, water reacts with alkali ions at the nonbridging oxygen (NBO) site to produce hydroxyl bonds and release alkali ions into solution, which increases the pH of the solution, as shown by equation (1). Next, the OH^- ion disrupts the siloxane bonds, as shown by equation (2). The ≡ Si-O-formed in equation (2) further reacts with H_2O producing an OH^- ion [equation (3)], which is free to repeat the reaction in equation (2). The release of Si from the glass into the contact solution, as silicic acid, occurs when BO bonds associated with Si are hydrolyzed, as shown by equations (5) and (6).

$$\equiv Si - O - M + H_2O \rightarrow \equiv Si - O - H + M^+ + OH^- \quad (1)$$

$$\equiv Si - O - Si \equiv + OH^- \rightarrow \equiv Si - O - H + \equiv SiO^- \quad (2)$$

$$\equiv Si - O^- + H_2O \rightarrow \equiv Si - O - H + OH^- \quad (3)$$

$$\equiv Si - O - M + H_3O^+ \rightarrow \equiv Si - O - H + M^+ + H_2O \quad (4)$$

$$= Si - OSi(OH)_3 + OH^- \rightarrow = Si - O^- + Si(OH)_4 \quad (5)$$

$$= Si - O - Si(OH)_3 + H_2O \rightarrow = Si - OH + Si(OH)_4 \quad (6)$$

As the corrosion front progresses inside the glass, more and more alkali ions are released from the glass into the solution and the solution, pH continues to rise. However, the increase in pH is counteracted by the release of a weak acid (silicic acid). The release of silicic acid increases sharply at pH > 9, as shown in Fig. 1. The initial rate of glass corrosion depends on the mass transport rate of H_2O or H_3O^+ to the alkali site and removal of alkalis out of the glass into the contact solution. In acidic pH, the ion-exchange reaction progresses at a much higher rate compared to the network hydrolysis reactions, as shown in Fig. 2.

As the reaction progresses, reaction layers are formed on the surface. The formation of reaction layers on the surface of the glass in contact with leachate plays a significant role in determining the leaching behavior of the glass components. Fig. 3 shows a schematic of the surface layers formed on the surface of the glass. The outermost surface layer is called the precipitation layer, while the innermost layer is called the diffusion layer. The layer sandwiched between the diffusion and precipitation layers is called the gel layer. The formation of the diffusion layer occurs through ion-exchange reactions shown by equations (1) and (2), while

the formation of the gel layer occurs through a hydrolysis reaction, shown by equations (3) and (4). As the glass corrodes and its components are released into solution, the leachate may become supersaturated with some components, leading to precipitation of the secondary phases on the surface of the glass or the walls of the test container.

The thickness of the gel layer remains constant if the pH of the contact solution does not change. If the contact solution becomes more alkaline, the Si dissolution increases, which may reduce the thickness of the gel layer. In a more complex system containing more than one glass-forming oxide such as B_2O_3 or Al_2O_3 (depending on the glass composition), the corrosion mechanism is further complicated by the release rate of various cations from the glass and their solubility in the contact solution.

The properties of the surface layer depend on the glass composition, contact solution chemistry, test parameters, and reaction time. The surface layers can provide a sink or reservoir for components in solution and act as a physical barrier to the transport of reactants and corrosion products. In addition, the surface layers can influence the chemical affinity of the glass reactions.

Depending on the test conditions, surface layers could either increase or decrease the corrosion rate. Chick and Pederson[9] showed that even though surface layers provide some transport barrier to glass reaction, the leaching behavior is controlled by the contact solution. Conradt[10] showed that surface layers in glass corroded in brine solutions (pH=5.7) at 120 and 200 °C had no effect on the corrosion rate, but when the glass was tested in 0.1 M NaOH (pH=12), glass corrosion was completely controlled by surface layers. Grambow and Strachan[11] tested simulated waste glass PNL 76-68 in deionized water and 0.001 M $MgCl_2$ solution and showed that the formation of surface layers in the $MgCl_2$ solution dominated the corrosion behavior of the

glass. The experimental evidence suggests that the surface layers provide a barrier to glass corrosion. However, the extent of this effect depends on the glass composition, characteristics of reaction layers, contact solution, temperature, and test conditions.

Surface layers that act as sinks reduce the concentration of corrosion species in the solution and increase the affinity for glass dissolution. The dissolution affinity is influenced by factors such as[12]

- Precipitated crystalline phases
- Amorphous silica phase(s)
- Gel layer
- Bulk glass components

GLASS DURABILITY MEASUREMENTS

Glass durability is not an intrinsic material property. Glass durability is dictated by the parameters controlled during testing. Typically the test is either dominated by the solution chemistry or the glass chemistry. The tests conducted using a low surface area/volume (SA/V) ratio are referred to as glass-dominated conditions. In this case, a monolithic sample is placed either in a large amount of water in closed system or in a periodic or continuous flowing condition. The corrosion behavior is not influenced by the glass components leached into the contact solution. The tests conducted using a high SA/V ratio are referred to as solution-dominated conditions. In this case, the contact solutions quickly attain saturation with the glass components, and the test results are dominated by the glass components leached into the contact solution. The glass components exceeding solubility limits in the solution often precipitate on the surface of the glass and lead to the formation

of secondary phases. Depending on their characteristics, these secondary phases could either increase or decrease the dissolution rate. These tests are used to provide accelerated corrosion of glasses.

The corrosion of glass is usually determined by measuring the amounts of various glass components that are released into the solution in contact with the glass. The components are released at different rates depending on the characteristics of the contact solution and the chemical composition of the glass. In alkali borosilicate glasses, alkali and boron are released at the fastest rate and are often used to measure corrosion. Boron and alkali have high solubility in solution and are not incorporated into the secondary phases that are formed on the surface of the glass. Boron is preferred over alkalis because, a boron release is more sensitive to reaction kinetics such as temperature and pH. However, to study the reaction mechanisms, additional components such as Al, Si, and others involved in the reactions are monitored. Table 1 shows different techniques and protocols used in determining glass durability. The test methods are generally categorized as static tests and dynamic tests. In static tests, the leachate is not refreshed or replaced, while in dynamic tests, the leachate is continuously or periodically refreshed or replaced.

Static Tests

The most widely used static tests to compare durabilities of various glasses, and the accepted test method for determining corrosion behavior, are Materials Characterization Center (MCC)–1 and MCC–3[13] and the PCT (ASTM C1285-97) durability test. In MCC–1, a monolithic glass sample is used in test solutions such as deionized water, brine, and silicate solution. The reference conditions include the SA/V ratio of 10 m^{-1} at 90 °C for 28 days. However, the conditions can be varied. The glass corrosion is determined by analyzing the concentration of the glass components in the leachate. The samples for the test are prepared by

fracturing, cutting, or grinding. The surface finish has a measurable effect on the corrosion rate. The rougher sample has a larger surface area and, therefore, a higher corrosion rate. The test sample and the contact solution are placed in a closed vessel, usually perfluoroalkoxy (PFA) Teflon®, and placed in a oven equilibrated at the test temperature. The PCT method is an ASTM standard (Test Method C 1285–97), a modified version of the MCC–3 test, and is exclusively developed to monitor the performance of the HLW glasses during production. This method uses a crushed sample, which provides a high SA/V ratio (2,000 m^{-1}) instead of the monolithic sample in MCC-1 (10 m^{-1}). The method details two versions of the test. The PCT-A method uses a crushed glass specimen with a particle size distribution between -100 and +200 (0.149 and 0.074 mm) mesh, placed in an airtight 304L stainless-steel vessel containing deionized water, which is ten times the mass of the crushed sample. This provides a SA/V of 2,000 m^{-1}, and the test is conducted at 90 °C for a fixed duration of 7 days. The normalized release concentration for element *i*, NC_i, in the leachate can be calculated by equation (7).

$$NC_i = \frac{C_i}{F_i} \tag{7}$$

where NC_i is in g-glass/m^3, C_i is the concentration of element i in solution in g/m^3, and F_i is the mass fraction of element *i* in glass. The PCT-B method allows variation in the SA/V ratio, particle size, leachate composition, temperature and time. This method is used for investigating the effect of various parameters on glass corrosion. The test uses either stainless steel or PFA Teflon® vessels. The high SA/V ratio accelerates saturation of glass components in the contact solution. A PCT can reach saturation in a few days while an MCC–1 test, which is a solution-dominated system (low SA/V ratio), may take significant time to reach saturation.

Dynamic Tests

The Soxhlet,[14] single-pass, flow-through (SPFT) test[15] and periodic replacement tests are widely used as dynamic tests. The Soxhlet test can be conducted over a temperature range of 90 to 250 °C. The test apparatus consists of a stainless steel reactor with a boiler supported by a condenser. The leaching vessel is located in the upper portion of the boiler. The water evaporating from the boiler is condensed in a reflux tube and is allowed to drip into the leaching vessel, which contains either a monolithic or crushed glass sample. The excess water from the leaching vessel overflows into the boiler. The corrosion rate is measured by periodically removing and analyzing the sample from the boiler. Since the leachate solution is recondensed, only deionized water can be used as a leachate solution. While the test allows studying a wide temperature and pressure range, the testing apparatus is quite complex. The test is useful where high flow rates are required.

The SPFT test is used to measure forward reaction rate. In this test, leachate solution is passed at a constant rate, using a peristaltic pump, into a cell containing a monolith or crushed glass. The solution leaving the cell is periodically collected and analyzed. The corrosion rate is determined by equation (8).

$$NR_{i,j} = (C_{i,j} - \overline{C}_{i,b})\frac{q_j}{f_i s_j} \tag{8}$$

where $NR_{i,j}$ is the normalized release rate of i^{th} element at the j^{th} sampling, q_j is the flow rate at the time period j in m^3/s, $C_{i,j}$ is the concentration of component i at the time period j, $C_{i,b}$ is the mean background concentration of component i, f_i is the mass fraction of component i in glass, and s_j is the surface area over the time period j-1 and j, m^2. In glasses, the corrosion rate increases to a maximum value as the flow rate

increases. This maximum corrosion rate is called the forward reaction rate. In this test, conditions such as leachate composition, temperature, and pH can be varied to measure the reaction characteristics.

In periodic replenishment tests, leachate solutions are periodically removed from the ongoing static tests. The static tests, such as MCC–1, MCC–3, and PCT, can be used to conduct periodic replenishment tests. The time of replenishment can be determined based on the aforementioned test conditions. The corrosion behavior of the glass depends on the amount of leachate replaced and the frequency of replacement.

The selection of a test method depends on the characteristics of the system under study. For example, if the interactions between the glass and contact solution are important without the influence of solution chemistry, tests such as MCC–1 or dynamic tests are recommended. If the effect of solution chemistry on the glass corrosion behavior is important, then tests such as PCT are more useful. Most of the literature data on glass durability are collected using either the MCC–1 or PCT method. Selecting the test method that duplicates the performance requirements (or meets the anticipated environmental conditions during use) of a glass is the key to conducting relevant tests.

PARAMETERS AFFECTING LEACHING BEHAVIOR

Test parameters such as SA/V ratio, flow rate, and temperature for a given method could limit the usefulness of the data for the desired application.

Effect of Surface Area to Volume Ratio

Glass dissolution initiates on the surface. The greater the surface area, the greater the dissolution of glass in the contact solution. However, the effect of surface area on glass dissolution is not linear. Ebert and Bates (1993) studied the dissolution of two reference Defense Waste Processing facility (DWPF) borosilicate glasses (SRL–131 and SRL–202) with SA/V ratios of 10; 2,000; and 20,000 m^{-1}. The results shown in Fig. 4 for SRL–131 glass indicate that B release cannot be linearly scaled as a function of SA/V·t. The higher, nonlinear release at the high SA/V ratio has been attributed either to the differences in the contact solution chemistry or mass transport effects. The changes in solution chemistry (i.e., the evolution of pH as a function of time) are shown in Fig. 5. Pederson[17] hypothesized that thicker surface layers are formed in tests with low SA/V ratio, which affects the mass transport to a greater degree compared to the thinner surface layers formed in high SA/V tests, which is responsible for higher B release from high SA/V samples. In addition, long-term tests can be affected by the changes in surface area. The release from the glass should be corrected to include the change in surface area of the glass with time due to pulverization from stresses, formation of secondary phases, or normal dissolution of glass. If the effects of solution chemistry, surface area, and nature of surface layers is not properly accounted for in the analysis, the extrapolation of short-term data to long-term behavior could be biased.

Effect of Flow Rates

In the dynamic tests, the leachate solution is continuously flushed at a given flow rate or periodically exchanged. The increase in ions released from the glass is counteracted by their removal through continuous or periodic leachate exchanges. The maximum corrosion will occur if the flow rate is such that the

components released from the glass do not exceed the solubility limit. Fig. 6 shows the normalized Na and Si release rates as a function of flow rate in SRL–131 glass. The curve shows two regions of leaching behavior. In region 1 the leach rate is proportional to flow rate up to 1 ml/hr, while, in region 2 beyond 10 ml/hr, the leach rate is nearly independent of flow rate. Fig. 7 shows the time dependence on corrosion at various flow rates. At high flow rates, the corrosion proceeds at a maximum rate that depends on the leachate composition, pH, and temperature but is independent of the flow rate. At a low flow rate, reaction rate decreases with time. The flow rate representing the maximum corrosion rate is referred to as a forward reaction rate.

Effect of Temperature

In general, the temperature dependence of reaction rate is expressed through an Arrhenius equation of the type shown by equation (9).

$$k = A \times \mathrm{e}^{\frac{E}{RT}} \tag{9}$$

where

- k — reaction rate constant or normalized release
- A — preexponential constant,
- E — activation energy,

T — temperature

R — gas constant.

Higher temperature is usually used as a method of accelerating the reactions, provided the reaction mechanism does not change over the range of temperature studied. Glass corrosion studies have been conducted from ambient temperatures to as high as 300 °C. However, most of the test methods are designed to study glass corrosion at 90 °C. Vernaz[20] studied the effect of temperature between 100 and 300 °C on R7T7 French HLW borosilicate glass. The glass samples were corroded for various time intervals. The data shown in Fig. 8 indicate two distinct corrosion mechanisms between 100 and 250 °C. The activation energy for the corrosion process was about 30 kJ/mol, while for a temperature greater than 250 °C, the activation energy increased to 150 kJ/mol. The corroded samples showed an increase in the thickness of the secondary phase layer from 1.5 to 30 μm when the temperature increased from 100 to 250 °C. The thickness of the secondary layer was almost 3 mm at 300 °C.

In addition, the leachate analysis showed that the effect of temperature on the release of various elements from the glass was not the same. Fig. 9 shows the distribution of activation energies observed in various nuclear waste and natural glasses. The reported activation energy for glass corrosion ranges from 22 to 150 kcal/mol.[6] The wide range of activation energies is attributed not only to the complex nature of the glass corrosion mechanism but also to the effects of glass composition, contact solution chemistry, reaction time, and temperature. Therefore, temperature data should be extrapolated with care to assure the corrosion mechanisms do not change over the extrapolation range.

Effect of Glass Composition

The chemical durability of a glass depends on its components. Because of the lack of a uniform testing and measurement approach to study durability-composition relationships, the data from various studies are difficult to compare quantitatively. Chemical durability-composition trends observed in various glass compositions are summarized here.

The chemical durability behavior of fused silica glass powder at 80 °C as a function of pH is shown in Fig. 1. Silica is a major component of all glass-forming systems. The data indicate that fused silica is fairly stable up to a pH of 9. Beyond pH 9, the network dissolution reactions, shown by equations (5) and (6), are responsible for Si dissolution from glass. In glass systems xNa$_2$O•10CaO•(90−x)SiO$_2$ containing alkali ions, Clark[21] showed that as Na concentration increases, the durability sharply decreases. In Na-Ca silicate glass, Das[22] showed that the rates of Na and Si release were different as a function of pH. The highest Na release rates were obtained in acidic conditions, while the highest Si release rates were obtained in alkaline solutions, as shown in Fig. 2. The chemical durability also depends on the particular alkali ion present. Dilmore[23] showed that 15K$_2$O•10CaO•75SiO$_2$ glasses leach at a higher rate than 15Na$_2$O•10CaO•75SiO$_2$ glass and that mixed alkali glasses such as (15−x)Na$_2$O•xK$_2$O•10CaO•75SiO$_2$ are more durable than either Na or K end-members. The presence of more than one type of alkali in the glass suppresses the alkali leaching from the glass. This behavior is called the mixed-alkali effect. Clark[21] showed that the addition of a divalent cation, such as Ca, in glass significantly improves durability. Similarly, Smets and Tholen[24] showed that in 20Na$_2$O•10MO•70SiO$_2$ glass (where M = Ca, Mg, or Zn), glass durability as measured by Na remaining in the glass decreased with the presence of Ca, Mg, and Zn, in order. This study also indicated that the most drastic changes were observed at low concentrations of the divalent ions.

In alkali borosilicate glasses, depending on the alkali/boron ratio, boron is either incorporated in the structure as tetrahedrally coordinated BO_4 species or trigonally coordinated BO_3 species. Adams and Evans[25] studied durability/composition relationships by reacting the glasses in a Na_2O-B_2O_3-SiO_2 system at 25 °C for 24 hours. Their study showed that the glass compositions that maximize the concentration of BO_4 tetrahedra tend to have the highest durabilities. Bunker[26] reached a similar conclusion in their durability study on a Na_2O-B_2O_3-SiO_2 glass system containing 60 mol% SiO_2 as a function of Na_2O/B_2O_3 ratio and as a function of SiO_2 for $Na_2O/B_2O_3 = 1$. They showed that in samples with Na_2O/B_2O_3 ratios $<<1$, Na and B were preferentially leached from the glasses. However, in glasses with $Na_2O/B_2O_3 \geq 1$, Na and B leached congruently in alkaline solutions. In addition, the glasses with $Na_2O/B_2O_3 = 1$ were orders of magnitude more durable than glasses with a lower or higher Na_2O/B_2O_3 ratio.

In short-term durability tests (less than 1 hr) of an alkali aluminosilicate [$20Na_2O \cdot xAl_2O_3 \cdot (1-x)SiO_2$] system, Smets and Lommen[27] showed the depth of the Na depletion decreased significantly with an increase in the Al_2O_3 concentration. The greatest change in depth of Na depletion was obtained with small amounts of added Al_2O_3, while for $x = 5$ or 10, the Na profile showed no measurable change. Similarly, for Li_2O-Al_2O_3-SiO_2 glasses, Dilmore[28] conducted durability tests at 100 °C for 41 days and showed that as the Al_2O_3 concentration increases in the glass, Li ions released in the leachate solution decreased. In alkali borosilicate glasses, depending on the alkali/alumina ratio, alumina is incorporated in the structure either as a tetrahedrally coordinated AlO_4 species (similar to B) or as a six-fold coordinated modifier in the absence of alkali ions in the glass structure. The improvement in durability is attributed to the formation of AlO_4 tetrahedra whose charge is balanced by alkali ions and forms an AlO_4Na bond, which is much stronger than NBO (≡Si-O-Na) bond.

16/89

In alkali iron silicates, the fraction of Fe^{3+} ions that are stabilized by alkali ions in tetrahedra coordination depends on the redox [Fe^{2+}/Fe^{3+} or $Fe^{2+}/Fe^{(total)}$] ratio in the glass. As the redox ratio increases or Fe^{3+} ions decrease, the number of FeO_4 tetrahedra decreases. Feng[29] studied the effect of the redox ratio [$Fe^{2+}/Fe^{(total)}$] on durability using the MCC–3 test on WV–205 simulated nuclear waste glass. The durability behavior is shown in Fig. 10. The normalized Na concentration increases sharply as the samples are reduced. The decrease in durability is attributed to the fact that, as the redox ratio increases, more alkali ions attach as NBO (≡Si-O-Na) to Si and fewer attach to the FeO_4 (FeO_4-Na) tetrahedra in the glass.

Feng[30] performed a study on WV–205 glass by systematically varying major components by small concentrations and measuring durability using the MCC–3 test at 90 °C at various time intervals up to 180 d in deionized water. Figs. 11, 12, and 13 show the effect of small additions of SiO_2, ZrO_2 and Al_2O_3, respectively, to WV–205 glass. The trends indicate that a significant increase in durability occurs with small additions of SiO_2, ZrO_2, and Al_2O_3, followed by a plateau region with a constant high durability. Feng[30] explained the effect based on the deficiency of network formers. In the nondurable glass region, the glasses can be considered deficient in network formers and, therefore, can be quickly attacked by water. Ellison[4] analyzed Feng[30] data and showed that WV–205 composition had a (Na+K+Li)/(B+Al) ratio of 1.8 and (Na+K+Li)/(B+Al+Fe) ratio of 1.3, which is significantly higher than one. Thus, small additions of network formers were able to significantly improve the durability of the glasses.

Nuclear waste glasses contain alkalis (Li, Na, K, Cs), oxides, divalent (Ca, Mg, Sr, Ba) oxides, Al_2O_3, B_2O_3, Fe_2O_3, SiO_2, ZrO_2, and many minor components. The interactions between components make the assessment of the composition/durability relationship challenging. Extensive work has been done to evaluate composition effects in nuclear waste glasses. The review of every waste glass system is beyond the scope of this report.

Table 2 summarizes the effect of various components on glass durability from several studies. The composition/durability studies indicate that the greatest improvements in durability result from the components that form the strongest bonds. For example, the durability of alkali silicate glass is improved by adding Al_2O_3, B_2O_3, Fe_2O_3, ZrO_2, or divalent cations (Ca, Mg, Zn, etc.) (shown in order of decreasing effect). The mechanism in each case is a formation of bonds stronger than the alkali-NBO bond in simple alkali silicate glass. The addition of Al_2O_3, B_2O_3, or Fe_2O_3 removes one NBO bond and, to compensate, alkali ions attach to AlO_4, BO_4, or FeO_4 tetrahedras.

Effect of Contact Solution

The nature of the solution in contact with glass has a significant effect on chemical durability. Feng and Pegg[31] leached simulated nuclear waste glass, WV–205, in the presence of various alkali nitrate solutions at 90 °C. Fig. 14 shows the effect of various alkali nitrates on the Si leach rate. The Si leach rates in various solutions were less than half those in deionized water. Reduced leaching in the presence of a salt solution is attributed to the ion-exchange reaction shown in equation (10)

$$\equiv \mathrm{Si} - \mathrm{O}^- M_2^+ + M_1^+ \leftrightarrow \equiv \mathrm{Si} - \mathrm{O}^- M_1^+ + M_2^+ \qquad (10)$$

where M_1 is the alkali cation in solution and M_2 is the alkali cation in glass. The ion-exchange reaction shown by equation (10) does not result in network hydrolysis as shown by equations (3) and (4), or increase the pH of the solution. However, the reaction competes with and suppresses the network hydrolysis reaction, thus lowering the Si dissolution rate. Barkett[32] showed that simulated nuclear waste glasses leached in Pacific

Coast seawater have almost two orders of magnitude lower Si and Al release rates and one order of magnitude lower B and alkali compared to the leach rates observed in deionized water. However, a recent study by Wickert[33] showed a significant increase in the dissolution rate of soda lime silicate glass with increasing NaCl concentration in the leachate. Wickert[33] attributed the increase in the leaching rate to the replacement of H ions by alkali, ions on the surface sites, which facilitates the access of aqueous medium in to Si-O-Si network.

Several studies have been conducted to determine the effect of container materials and corrosion products on glass dissolution behavior. McVay and Buckwalter[34] and Burns[35] studied the effect of metals on glass dissolution behavior. While the former showed higher glass dissolution in the presence of ductile iron, the latter showed no significant effect on glass dissolution from 304L stainless steel and 409 and 430 ferrite steels. In addition, Burns[35] showed that A516 carbon steel had a significant detrimental effect on glass dissolution. Inagaki,[36] Bart,[37] and Werme[38] studied the effect of magnetite on glass dissolution behavior. Magnetite is considered a primary corrosion product, and for many disposal systems these studies showed that glass dissolution is enhanced by the presence of magnetite. Werme[38] also studied the effect of FeOOH and concluded that glass dissolution is higher in the presence of FeOOH than in the presence of the same amount of magnetite. These studies clearly establish the effect of magnetite and FeOOH on enhancing glass dissolution. Pan[39] studied the behavior of simulated waste glass samples from WVDP and DWPF by subjecting them to long-term leaching tests in the presence of $FeCl_2$ and $FeCl_3$ at 90 °C, to simulate a corroded waste package (WP) environment. Ferrous and ferric chlorides Fig. 15 were selected because chloride is the primary ion responsible for WP corrosion. Results, as indicated in, showed substantially higher initial normalized release for B and alkali, approximately a factor of 50 to 70 times greater than those in deionized water in 0.25-M $FeCl_3$ solutions. The initial leaching rate (Fig. 16) for B and alkali was found to be

pH-dependent and decreased as the leachate pH was increased. While the leach rate for Si did not show any significant change in the pH range studied, the leach rate for Al showed a minimum. The minimum for the leach rate of Al occurred at different pH values. The study indicates that elements in the glass matrix are released incongruently.

As indicated by several studies, the contact solution has a significant effect on the glass dissolution. Studies, however, fail to indicate specific trends in the dissolution behavior in the presence of various salts or components in the contact solution.

CHEMICAL DURABILITY MODELS

General Chemical Durability Models

Several attempts have been made to correlate chemical durability and glass composition. In this section, proposed empirical and thermodynamic relationships for durability behavior are reviewed. The models discussed assume that the glass is homogeneous and crystal free. In addition, the models only apply to normalized release measured in static tests of fixed duration, and there is no correlation between data collected using static tests and long-term durability. Static tests can only verify product consistency and can not be regarded as an accurate measure of relative durability of a glass.

The free energy of hydration (FEH) model was initially developed by Paul[2] for simple alkali silicate glasses and later extended by Jantzen[3] to complex borosilicate-based waste glasses. FEH relates the thermodynamic properties of glasses to their dissolution rates as measured in short-term, closed-system tests such as MCC–1

and PCT. FEH treats glasses as solids composed of mechanical mixtures of silicate and oxide components as shown in Table 3. The net free energy change (ΔG_{hyd}) is calculated as

where $(\Delta G_{hyd})_i$ is the free energy change in kcal/mol of the thermodynamically most stable hydration reaction of the structurally associated silicate and oxide of component *i* having mol fraction x_i. The model assumes that the choice of structural units is adequate and that free energy of mixing of the components in the glass can be neglected. The original approach of Paul[2] assumed that the silicate and borate components of a glass hydrate to silicic and boric acid. However, for low-durability glasses where alkali released from the glass

$$\Delta G_{hyd} = \Sigma x_i \bullet (\Delta G_{hyd})_i \tag{11}$$

increases the pH of the solution >9.5, the solubilities of silica and borate rapidly increase. Therefore, additional contribution to the FEH should be included to account for silicic and boric acid dissolution at pH 9.5. The additional contribution is calculated by

$$\Delta(\Delta G_{hyd}) = 1.364\left[-\log\left(1+\frac{10^{-10}}{10^{-pH}}+\frac{10^{-21.994}}{10^{-2pH}}\right)\right] \text{ for } \quad H_2SiO_3 \tag{12}$$

and

$$\Delta(\Delta G_{hyd}) = 1.364\left[-\log\left(1+\frac{10^{-9.18}}{10^{-pH}}+\frac{10^{-21.89}}{10^{-2pH}}+\frac{10^{-35.69}}{10^{-3pH}}\right)\right] \text{ for } \quad H_2BO_3 \tag{13}$$

Linear relationships shown by equations (12) and (13) were developed between the logarithmic normalized release from the glass in g-glass/m^2 and the calculated ΔG_{hyd} including the effect of silicic and boric acid. Fig. 17 shows normalized B and Si release for more than 300 data points collected using the MCC–1 test for 28 days at 90 °C as a function corrected FEH. The relationship statistically showed that release rate was better correlated with corrected FEH than uncorrected FEH. The more negative the FEH, the less durable the glass. Glasses, such as natural obsidians, tektites, basalts, silica, pyrex, window glass, and ancient Roman and Islamic glasses, were included in the study. The relationship between the Si and B normalized release and the adjusted ΔG_{hyd} is

$$\log(NL_{Si}) = -0.2240\Delta G_{hyd} - 0.0448 \qquad r^2 = 0.73 \tag{14}$$

$$\log(NL_{B}) = -0.2795\Delta G_{hyd} + 0.2147 \qquad r^2 = 0.59 \tag{15}$$

where NL_i is the normalized release in g-glass/m^2 for component *i*. Jantzen[41] refined the FEH model for predicting durabilities of the HLW glasses produced at DWPF. The refined thermodynamic hydration energy reaction model (THERMO) calculates the FEH, ΔG_f, as

$$\Delta G_f = \Delta G_p + \Delta G_a^{WA} + \Delta G_a^{SB>11} + \Delta G_a^{SB>12} \tag{16}$$

where, ΔG_p is the FEH, in kcal/100 gm-glass, represented by equation (11), and the $\Delta G_a{}^i$ terms are the contributions from the accelerated dissolution reactions. The $\Delta G_a{}^{WA}$ represents the weak acid (WA) disequilibrium effect, and $\Delta G_a{}^{SB>11}$ and $\Delta G_a{}^{SB>12}$ terms represent strong base effects at pH >11 and >12. The $\Delta G_a{}^{WA}$ is sum of contributions from equations (12) and (13). The relationship between the normalized release (g/L) and the ΔG_f was developed using the PCT-A (7 d at 90 °C) as

$$\log[NL_{Na}(g/L)] = -0.0981\Delta G_f - 1.448 \qquad r^2 = 0.88 \tag{17}$$

$$\log[NL_{B}(g/L)] = -0.104\Delta G_f - 1.535 \qquad r^2 = 0.86 \tag{18}$$

Note that the FEH and THERMO not only use different units for data analysis but also use different test methods. A step-by-step method for calculating FEH for the THERMO model is provided in Jantzen.[41]

For vitrified HLW, Hrma[42] conducted a multiyear statistically designed component variability study (CVS) to characterize the relationship between composition and properties. Table 4 shows target composition and upper and lower limits for various components in the study. The target composition, HW–39–4, is based on the proposed Hanford HLW glass composition for the NCAW waste (now known as envelope B/D waste). Glass durability was measured on 120 glasses using 28 days MCC–1 and 7 d PCT methods. Compositional dependence on normalized release was determined by the first-order mixture models as

$$NR = \sum_{1}^{10} b_i x_i \tag{19}$$

where

NR — the normalized release in g/m^2

x_i — mass fraction

b_i — regression coefficients for component i

The estimated regression coefficients for B, Si, Na, and Li are shown in Tables 5 and 6 for MCC–1 and PCT data, respectively. For MCC–1 data, seven data points representing high B release were removed from the analysis. Their removal was attributed to nonlinear or interactive effects of components, which cannot be addressed by first-order mixture models. The r^2 statistics indicate that the first-order mixture model for MCC–1 data provides some predictive ability. Based on the regression coefficients provided in Table 5, a component effects plot using normalized boron release was developed centered around composition HW–39–4 (Fig. 18). The analysis predicts that normalized B release is increased by Li_2O, Na_2O, and B_2O_3 (in the order written) and decreased by Al_2O_3 and SiO_2. For the PCT data set, no data points were removed. The r^2 values for the PCT data set were higher than the MCC–1 data set, indicating that the first-order mixture model for PCT data provides better predictive ability than MCC–1 data. Based on the regression coefficients provided in Table 6, a component effects plot using normalized boron release was developed centered around composition HW–39–4, shown in Fig. 19. The analysis predicts that normalized B release is increased by Li_2O, B_2O_3, and Na_2O and decreased by Al_2O_3 and SiO_2. The MCC–1 and PCT data were analyzed using first-order mixture model terms along with several second-order terms selected using statistical variable selection techniques to improve the relationship between normalized release for B, Si, Na, and Li, and composition. The second-order mixture model provided a slightly better fit than the corresponding first-order mixture models.

Feng and Barkatt[43] developed a structural bond strength (SBS) that assumes the dissolution of glass is controlled by the breaking of network bonds such as Si-O-Si. The energy of formation that represents an average structural strength of the glass is calculated by equation (20).

$$\Delta H = \sum_i x_i \Delta H_i \tag{20}$$

where ΔH is the total energy of formation, and ΔH_i is the energy of formation for component i having mol fraction x_i in glass. The methodology of calculating the energy of formation of various glass components is discussed in reference 43. The model was applied to various nuclear waste glasses from West Valley, DWPF, and PNNL; commercial glasses, such as aluminosilicate and soda lime silica; and natural glasses such as basalts and tektites. The tests were conducted using the modified MCC–3 test. The MCC–3 test is a closed-system test using a crushed sample. Linear relationship shown by equations (21) and (22) were developed between the logarithmic normalized release from the glass and the calculated ΔH.

$$\log(\mathrm{NL}_{\mathrm{B-7day}}) = -0.0193\Delta H + 5.2667 \qquad r^2 = 0.705 \tag{21}$$

$$\log(\mathrm{NL}_{\mathrm{B-28day}}) = -0.02865\Delta H + 8.358 \qquad r^2 = 0.723 \tag{22}$$

Ellison[4] used an independent data set consisting of normalized release data using the MCC–1 test at 90 °C for 28 days for 300 glasses and evaluated prediction capabilities of the FEH, THERMO, CVS, and SBS models. The data set included waste glasses (alkali boroaluminosilicate, alkali borosilicate, alkali aluminosilicate, and alkali lime silicates), natural glasses, and historical glasses. Results showed that FEH provided the best correlation between glass composition and durability among various models. FEH provided the best results for alkali boroaluminosilicate glasses having high mass losses, but provided poor correlation for highly durable glasses. For the SBS model, regression analysis showed the best correlation for alkali

boroaluminosilicate glasses ($r^2 = 0.80$) and the worst for alkali borosilicate glasses ($r^2 = 0.05$). Compared to the FEH model, the SBS model provided a better correlation for predicting normalized release for highly durable glasses. Neither the SBS nor the FEH models provided a good correlation for alkali borosilicate glasses.

Tovena[44] used normalized release data for 32 waste glass samples (6 R7T7 and 26 SON) to test the FEH and SBS models. Both the FEH and SBS models provided satisfactory approximation of initial release rate. However, the models underpredicted the normalized release rate for glasses containing >15 wt% B_2O_3 with little Al_2O_3. This departure was attributed to the phase separation and complete dissolution of the borate phase in the absence of Al_2O_3.

The thermodynamic, structural, and empirical models reviewed in this chapter were developed for a specific range of glass compositions and glass components. Even though the applicability of these models can be extended to other wastes, as shown by Ellison[4] and Tovena,[44] the user is cautioned to perform a careful and rigorous evaluation prior to using any model for predicting normalized release from the glass. In addition, the models predict glass performance under given test conditions at a single time; therefore, the results cannot be used for predicting time-dependent durability behavior.

Long-Term Chemical Durability Models

The release of components from glass follows a complex nonlinear behavior as a function of time. The behavior is a combination of glass composition effects, changes in solution chemistry with time, formation of secondary phases, and temperature. The long-term corrosion behavior can be divided into three distinct stages

as reviewed by Ellison.[4] In stage I, referred to as the short-term stage, the chemical potential gradient between the glass components and local environment is the steepest. The glass components are released into the local environment at a comparatively high rate. The soluble components, such as boron and alkalis, are released at a higher rate compared with components such as silica and aluminum oxide. This higher release rate results in the formation of a layer on the glass surface depleted of soluble components, compared with the bulk glass. This layer is often called the altered surface layer. In stage II, the intermediate stage, the corrosion rate decreases as the concentration of reaction products, particularly silica, increases in the solution that is in close contact with the glass. In addition, the reaction products in the altered surface layer reach saturation concentration of their crystalline phases and result in the formation of secondary phases, such as zeolites and clays. In stage III, the long-term stage, glass corrosion rate is further affected because of the reprecipitation of secondary phases that exceed solubility limits at the altered zone. Physical processes, such as crystallization, cracking, or exfoliation of the altered surface layers, that occur in stage III, could influence the glass corrosion rate, as well as the release and transport of colloids and radionuclides. The change in dissolution rate also depends on the identity, distribution, and surface area of the secondary phases. In most cases, the dissolution rate increases as a result of crystallization, exfoliation, and cracking of the altered surface layers. The transition from one stage to another is dependent on the glass composition and the local environment. A highly durable glass may take months to years to reach stage II, whereas a nondurable glass may reach stage II within hours or days.

The long-term dissolution models use a rate equation consistent with the transition state theory[5]

$$\frac{dn_i}{dt} = An_i k_r \prod_j a_j^{-n} \left(1 - e^{\left(-\frac{A_f}{\sigma RT}\right)}\right) \tag{23}$$

where

n_i — is the number of mols of species i in solution released from the glass

t — time

A — reactive surface area of glass

v_i — concentration of species i in the glass

k_r — rate coefficient for the rate-limiting reaction for glass dissolution

$\prod_j a_j^{-n}$ — the product of the activities (concentrations) of dissolved aqueous species, that contributes to the activated complex of the rate-limiting microscopic dissolution reaction

A_f — reaction affinity, defined as $RT\ln(Q/K)$, where Q is the activity product and K is the equilibrium constant for the rate-determining glass dissolution reaction

σ — a stoichiometric factor that relates the rate-controlling microscopic reaction to the overall solid dissolution reaction (usually it is assumed $\sigma = 1$)

R — gas constant

T — temperature in kelvin.

Equation (23) implies that, at equilibrium, there is a reversible dissolution reaction. Since the glass is considered as thermodynamically metastable, the rate law cannot be applied to the overall glass dissolution but to some rate-limiting microscopic reversible reaction. Several parameters shown in equation (23) are not known either from theory or experiments. Therefore, the rate equation is simplified to the form

$$\frac{dn_i}{dt} = An_i k(\mathrm{pH})\left(1-\left(\frac{Q}{K}\right)^r\right)^\sigma \tag{24}$$

Equation (24) is commonly used for determining release rate. The parameters k, K, r, and σ are determined by fitting experimental data. Grambow further simplified equation (24) to include only silica in the affinity term and expressed glass dissolution rate as

$$R_m = k_+\left(1-\left(\frac{a_{SiO_2(aq)}}{K}\right)\right) + R_{final} \tag{25}$$

where

R_m — matrix dissolution rate

k_+ — rate coefficient

$a_{SiO2(aq)}$ — the activity of aqueous silica at the reacting surface

K — glass saturation activity

R_{final} — residual rate after silica saturation is achieved

The parameters K and k_+ are regressed from experimental data. Geochemical modeling codes, such as PHREEQE/GLASSOL, EQ3/6, DISSOL, REACT, and LIXIVER, use an expression shown by equations (24) and (25). Grambow's model has been applied to several closed- and open-system dissolution

tests for a variety of glass compositions. In most cases, the model predicts observed trends and agrees with measured solution compositions to within a factor of two or three. The model, however, requires that parameters such as K and k_+ be determined for each glass composition. In addition, the release of components can only be modeled assuming congruent dissolution; the model does not provide a mechanistic basis for predicting the long-term dissolution rate of glasses. The long-term models have no capability to predict how the rate may change as the environmental parameters change during the lifetime.

GLASS BEHAVIOR IN THE REPOSITORY ENVIRONMENT

Several long-term HLW glass corrosion studies have been conducted in the previous 20 years on simulated glasses doped with plausible radionuclides, and fully radioactive glasses. Drip tests, designed to simulate slow flow through the breached canisters, have been used by Fortner and Bates[45] and Fortner[46] to study the long-term performance of actinide-doped WVDP and DWPF HLW glasses. The long-term PCT-B, designed to simulate fully immersed conditions, has been used by Ebert and Tam[47] to study the long-term performance of DWPF glasses. In addition, vapor hydration tests (VHT), designed to replicate a natural alteration process, are used by Luo[48] to compare the dissolution behavior of DWPF glasses with that of naturally occurring basalt glasses.

The dissolution rate of the HLW glass decreases as the groundwater environment in close contact with the WPs becomes saturated with glass matrix components, such as silica. Even though the glass corrosion studies discussed previously confirmed that net dissolution rate decreases as the surrounding environment becomes rich in HLW glass matrix components, the drip test studies show a steep increase in radionuclide release rate for Pu and Am after 400 weeks. The steep increase in radionuclide release rate was attributed to the spalling

of radionuclide-containing colloids from the exposed HLW glass surface. The HLW glass corrosion models currently proposed do not account for such excursions in corrosion behavior, although they can have a significant effect on radionuclide release.

Long-term corrosion studies of HLW glasses indicate formation of secondary phases on the exposed surface of the HLW glasses. This process is dependent on the external environment. Long-term PCTs in J-13 water show formation of clay, Ca-phosphate, and (Th, U, and Ca) titanate as secondary phases,[49] whereas, the VHTs show accumulation of clay, zeolites, Ca-silicates, weeksite, and K-feldspar as secondary phases.[49] The formation of different phases under diverse test conditions is attributed to varying solution chemistries. The formation of secondary phases may also be influenced by the corroding container materials. Secondary minerals play an important role in radionuclide release because they can incorporate low-solubility radionuclides, such as Pu and Am, and control their solubility limits. They may also act to block the reactive surface area of the primary phase.

It is important that the long-term radionuclide release rate in the corrosion models includes the influence of stage III behavior. Experimental data on the formation of secondary phases under anticipated repository conditions are necessary if the contribution of the HLW glass to the estimated receptor dose is significant. If the models are simply based on experimental dissolution data for stages I or II that exhibit significant retention of radionuclides in the secondary phases, evaluation of the long-term radionuclide release rates could be erroneous.

Natural analog studies, coupled with experimental data and geochemical modeling, provide other methods of gaining confidence in predicting long-term corrosion behavior of glasses. Natural analog studies are useful

in evaluating the merits of extrapolating short-term experiments to longer time frames. Several natural glasses, especially basalt, have compositions comparable to the HLW glasses and have been subjected to conditions similar to those expected in the proposed Yucca Mountain repository.[50] The characterization of secondary phases formed on these natural glasses can provide insights into the long-term dissolution behavior of HLW glasses.

A recent study by Luo[48] compared the formation of secondary phases in the naturally occurring Hawaiian basaltic glasses with the results of VHTs conducted for 7 years on simulated basaltic and HLW borosilicate glasses. Luo[48] concluded that secondary phases formed on both simulated natural glasses and HLW borosilicate glasses were similar to secondary phases observed in naturally occurring basaltic glasses, and VHTs could be used to simulate naturally occurring conditions.

Field data on naturally occurring glasses, combined with experimental data and models on dissolution of HLW glasses, could be useful to demonstrate that long-term dissolution behavior under repository conditions can be represented by extrapolation of results from short-term laboratory tests. Such data can be important to supplement and support the validity of the existing glass-dissolution data generally obtained by short-term experiments.

SUMMARY

When a glass comes in contact with an environment, such as flowing or stagnant groundwater, corrosive gases and vapors, or aqueous solutions, chemical reactions occur at the surface, which then spread to the whole of the glass, depending on its composition, the pH of the solution, and the temperature of the

environment. Several studies have focused on understanding two aspects of nuclear waste glasses. First, the ability to produce glasses to meet production specifications based on short-term tests and second, predicting the long-term dissolution behavior of glasses on the of 10,000 years or more. Several methods have been developed to perform accelerated testing to determine corrosion behavior of glasses. Since glass corrosion is not an intrinsic property of the materials, the observed dissolution behavior depends on the test conditions and test methods. A careful evaluation is required in drawing conclusions regarding the chemical durability of a glass based solely on data. A few test methods that form the basis of current understanding are discussed, including relationships between glass composition and environment (pH, temperature, and nature of solution) as a function of time. The processes involved in glass corrosion include ion-exchange, water diffusion, hydrolysis, and precipitation. Even though dissolution may start by simple ion-exchange or the hydrolysis reaction, the simultaneous occurrence of stated processes is not uncommon.

The initial reaction on the glass surface is dominated by the initial pH of the contact solution. As the reaction progresses, reaction layers are formed on the surface. The formation of reaction layers on the surface of the glass in contact with leachate plays a significant role in determining the leaching behavior of the glass components. As the glass corrodes and its components are released in the solution, the leachate may become supersaturated with respect to some components, leading to precipitation of the secondary phases on the surface of the glass or the walls of the test container. The thickness of the gel layer remains constant provided the pH of the contact solution does not change. If the contact solution becomes more alkaline, the Si dissolution increases, which may reduce the thickness of the gel layer. In a complex system containing more than one glass forming oxides, such as B_2O_3 and Al_2O_3 (depending on the glass composition), the corrosion mechanism is further complicated by the release rate of various cations from the glass and their solubility in the contact solution. The properties of the surface layer depend on glass composition, contact

solution chemistry, test parameters, and reaction time. The surface layers can provide a sink or reservoir for components in solution and act as a physical barrier to the transport of reactants and corrosion products. In addition, surface layers can influence the chemical affinity of the glass reactions.

The selection of a test method depends on the characteristics of the system to be studied. For example, if the interactions between the glass and contact solution are important without the influence of solution chemistry, tests such as MCC–1 or dynamic tests are recommended. If the effect of solution chemistry on the glass corrosion behavior is important, tests such as PCT are more useful. Most of the literature data on glass durability was collected using either the MCC–1 or the PCT method. Test parameters such as SA/V ratio, flow rate, and temperature for a given method could limit the usefulness of the data for the desired application.

The chemical durability of a glass depends on its components. Because of the lack of a uniform testing and measurement approach to study durability-composition relationships, data from various studies are difficult to compare quantitatively. The composition/durability studies indicate that the greatest improvements in durability result from adding components that form the strongest bonds. For example, the durability of alkali silicate glass is improved by adding Al_2O_3, B_2O_3, Fe_2O_3, ZrO_2, or divalent cations (Ca, Mg, Zn). The mechanism in each case is formation of bonds stronger than the alkali-NBO bond in simple alkali silicate glass. In addition, the nature of the solution in contact with glass has a significant effect on chemical durability.

Several attempts have been made to correlate chemical durability and glass composition. The models assume that the glass is homogeneous and crystal free. The thermodynamic, structural, and empirical models discussed in this report were developed for a specific range of glass compositions and glass components.

Even though the applicability of these models can be extended to other wastes, the user is cautioned to perform a careful and rigorous evaluation prior to using any model for predicting normalized release from the glass. In addition, the models predict glass performance under given test conditions at a single time; therefore, the results cannot be used for predicting time-dependent durability behavior. The long-term dissolution models use rate equations consistent with the transition state theory. Grambow's model has been applied to several closed- and open-system dissolution tests for a variety of glass compositions. In most cases, the model predicts observed trends and agrees with the measured solution compositions to within a factor of two or three. However, the model does not provide a mechanistic basis for predicting the long-term dissolution rate of glasses. The long-term models have no capability to predict how the rate may change as the environmental parameters change during the performance period for the glass.

REFERENCES

1. R.G. Newton: *Glass Technology*, 1985, 26, (1), 21–28.

2. A. Paul: *Journal of Material Science*, 1977, 12, 2,246–2,268.

3. C.M. Jantzen: *Journal of the American Ceramic Society*, 1992, 75, (9), 2,433–2,448.

4. G. Ellison, J.J. Mazar, and W.L. Ebert: "Effect of glass composition on waste form durability: a critical review," Report ANL–94/28, Argonne, IL, Argonne National Laboratory, 1994.

5. W.L. Bourcier: "Critical review of glass performance modeling," Report ANL–94/17, Argonne, IL: Argonne National Laboratory, 1994.

6. U.S. Department of Energy: "High-level waste borosilicate glass: a compendium of corrosion characteristics," (Volumes 1, 2, and 3), Report DOE–EM–0177, Washington, DC, Office of Waste Management, U.S. Department of Energy, 1994.

7. Ernsberger: *Physics Chem. Glasses*, 1980, 21, 146–149.

8. A. Paul: "Chemistry of Glass," 1982. New York, Chapman and Hall, Ltd.

9. L.A. Chick and L.R. Pederson in Proc. Conf. "MRS Symposium Proceedings Vol. 26," Pittsburgh, PA, 1984, Materials Research Society, 635–642.

10. R. Conradt, H. Roggendorf, and H. Scholze in Proc. Conf. "MRS Symposium Proceedings Vol. 50," Pittsburgh, PA, 1985, Materials Research Society, 203–210.

11. B. Grambow and D.M. Strachan in Proc. Conf. "MRS Symposium Proceedings Vol. 26," Pittsburgh, PA, 1984, Materials Research Society, 623–634.

12. Feng, X in Conf. Proc. "MRS Symposium Proceedings Vol. 333," Pittsburgh, PA, 1994, Materials Research Society, 55–67.

13. U.S. Department of Energy: "Nuclear waste materials handbook—test methods," Report DOE/TIC–11400, Pacific Northwest National Laboratory, Richland, WA, 1982.

14. F. Delage and J.L. Dussossoy in Proc Conf. "MRS Symposium Proceedings Vol. 212," Pittsburgh, PA, 1991, Materials Research Society, 41–47.

15. B.P. McGrail, W.L. Ebert, A.J. Bakel, and D.K. Peeler: *Journal of Nuclear Materials*, 1997, 249, 175–189.

16. W.L. Ebert and J.K. Bates: *Nuclear Technology*, 1993, 104, (3), 372–384.

17. L.R. Pederson, C.Q. Buckwalter, G.L. McVay, and B.L. Riddle in Proc. Conf. "MRS Symposium Proceedings Vol. 15," Pittsburgh, PA, 1983, Materials Research Society, 47–54.

18. L.L. Hench, D.E. Clark, and A.B. Harker: *Journal of Material Science*, 1986, 21, 1,457–1,478.

19. R.B. Adiga, E.P. Akomer, and D.E. Clark in Proc. Conf. MRS Symposium Proceedings Volume 44,"1985, Pittsburgh, PA, Materials Research Society, 45–54

20. E.Y. Vernaz, J.L. Dussossoy, and S. Fillet in Proc. Conf. "MRS Symposium Proceedings Vol. 112," 1988, Pittsburgh, PA, Materials Research Society, 555–563.

21. D.E. Clark, M.F. Dilmore, E.C. Ethridge, and L.L. Hench: *Journal of American Ceramic Society*, 1976, 59, 62–65.

22. C.R. Das: *Journal of American Ceramic Society* 1980, 63, 160–165.

23. M.F. Dilmore, D.E. Clark, and L.L. Hench: *Journal of the American Ceramic Society*, 1978, 61, 439–443.

24. B.M. Smets and M.G.W. Tholen: *Journal of American Ceramic Society*, 1984, 67, 281–284.

25. P.B. Adams and D.L. Evans: "Borate glasses: structure, properties, applications," 1978, New York, Plenum Press.

26. B.C. Bunker, G.W. Arnold, D.E. Day, and P.J. Bray: *Journal of Non-Crystalline Solids*, 1986, 87, 226–253.

27. B.M. Smets and T.P.A. Lommen: *Physics and Chemistry Glasses 23*, 1982, 83–87.

28. M.F. Dilmore, D. E. Clark, and L.L. Hench: *Journal of the American Ceramic Society*, 1978, 57, 339–353.

29. X. Feng, A.A. Barkett, and T. Jiang in Proc. Conf. "MRS Symposium Proceedings Vol. 112," 1988, Pittsburgh, PA, Materials Research Society, 673–683.

30. X. Feng, I.L. Pegg, A.A. Barkatt, P.B. Macedo, S.J. Cucinel, and S.Lai: *Nuclear Technology*, 1989, 85: 334–345.

31. X. Feng, and I.L. Pegg: *Physics and Chemistry Glasses*, 1994, 35, (2).

32. A.A. Barkatt, E.E. Saad, R. Adiga, W. Sousanpour, A.L. Barkett, M.A. Adel-Hadadi, J.A. O'Keefe, and S. Alterescu: *Appl. Geochem*, 1989, 4, 593–603.

33. C.L. Wickert, A.E. Vieira, J.A. Dehne, X. Wang, D.M. Wilder, and A. Barkatt: *Physics and Chemistry of Glasses*, 1999, 40, (3), 157–170.

34. G.L. McVay and C.Q. Buckwalter: *Journal of the American Ceramic Society*, 1983, 66, (3), 170–174.

35. D.B. Burns, B.H. Upton, and G.G. Wicks: Interactions of SRP waste glass with potential canister and overpack metals. *Journal of Non-Crystalline Solids*, 1986, 84, 258–267.

36. Y. Inagaki, A. Ogata, H. Furuya, K. Idemistu, T. Banba, and T. Maeda in Proc Conf. "MRS Symposium Proceedings Vol. 412," 1996, Pittsburgh, PA, Materials Research Society, 257–264.

37. G. Bart, H.U. Zwicky, E.T. Aerne, T.H. Graber, D. Z'Berg, and M. Tokiwai in Proc. Conf. "Ceramic Transactions Volume 84," 1997, Westerville, OH, American Ceramic Society, 459–470.

38. L. Werme, I.K. Bjorner, G. Bart, H.U. Zwicky, B. Grambow, W. Lutze, R.C. Ewing, and C. Magrabi: *Journal of Materials Research*, 1983, 5, (5), 1,130–1,146.

39. Y.-M. Pan, V. Jain, M. Bogart, and P. Deshpande in Proc. Conf. "Ceramic Transactions Volume 119," St. Louis, MO, 2000, American Ceramic Society, in press.

40. V. Jain and Y.-M. Pan in Proc. Conf. "Atalante 2000," Avignon, France, 2000, in press.

41. C.M. Jantzen, J.B. Pickett, K.G. Brown, and T.B. Edwards. U.S. Patent No. 5,846,278. Issued on December 8, 1988.

42. P.R. Hrma,, G.F. Piepel, M.J. Schweiger, D.E. Smith, D.-S. Kim, P.E. Redgate, J.D. Vienna, C.A. LoPresti, D.B. Simpson, D.K. Peeler, and M.H. Langowski: "Property/composition relationships for hanford high-level waste glasses melting at 1,150 °C," Volume 1, Chapters 1–11, PNL–10359, Pacific Northwest National Laboratory, Richland, WA, 1994.

43. X. Feng and A. A. Barkatt in Proc. Conf. "MRS Symposium Proceedings Vol. 112," 1988, Pittsburgh, PA, Materials Research Society, 543–554.

44. I. Tovena, T. Advocat, D. Ghaleb, E. Vernaz, and F. Larche in Proc. Conf. "MRS Symposium Proceedings Vol. 333," 1994, Pittsburgh, PA, Materials Research Society, 595–602.

45. J.A. Fortner and J.K. Bates in Proc. Conf. "MRS Symposium Proceedings 412," 1996, Pittsburgh, PA, Materials Research Society, 205–211.

46. J.A. Fortner, S.F. Wolf, E.C. Buck, C.J. Mertz, and J.K. Bates in Proc. Conf. "MRS Symposium Proceedings Vol. 465," 1997, Pittsburgh, PA, Materials Research Society: 165–172.

47. W.L. Ebert and S.W. Tam in Proc. Conf. "MRS Symposium Proceedings Vol. 465," 1997, Pittsburgh, PA, Materials Research Society, 149–156.

48. J.S. Luo, W.L. Ebert, J.J. Mazer, and J.K. Bates in Proc. Conf. "MRS Symposium Proceedings Vol. 465," 1997, Pittsburgh, PA, Materials Research Society, 157–163.

49. J.K. Bates. "Distribution and stability of secondary phases," Workshop on Preliminary Interpretations Waste Form Degradation and Radionuclide Mobilization Expert Elicitation Project, 1998, San Francisco, CA.

50. R.C. Ewing W. Lutze, and A. Abdelouas in Proc. Conf. " XVIII International Congress on Glass (CD Rom Edition)," 1998, Westerville, OH: American Ceramic Society.

Table 1. Summary of leach test methods[6]

Name of Test	Temperature (°C)	Leachant	Flow Rate	Sample Description	Reference
Soxhlet	50–100	Distilled water	1.5 cm^3/min	Plate, SA = 3 cm^2	1
Modified soxhlet	35–100	Distilled water	Variable	Grains or plate SA = Variable	2
Hot-cell soxhlet	100	Distilled water	80 cm^3/hr	Beads/plates/chips SA = Variable	3
MCC–5 soxhlet	100	Distilled water	~1.5 cm^3/min	Plate, S = 4 cm^2	4
Soxhlet (PNC)	70,100	Distilled water	60–225 cm^3/hr	Bar, SA = 2 cm^2	5
HIPSOL (HT soxhlet)	100–300	Distilled water	100–900 cm^3/hr	Powder or block	6
IAEA	25	Distilled water	Periodic replacement	Cylinder with exposed surfaces	7
ISO Buffer	23–100	Distilled water, buffers, and seawater	Periodic replacement	Monoliths	7
Powder (P1)	95–200	Distilled water	Periodic replacement	Powder, 100–200 μm	8
Powder (P2)	40–100	Deionized water	Daily replacement	Powder, 100–150 mesh	9
MCC–4	40, 70, 90	Distilled water and reference groundwater	0.1–0.001 cm^3/min	Plate, SA = 4 cm^2	4
Low-flow	25–90	Distilled water	1 cm^3/wk	Plate, SA = 3 cm^2 (radiotracers)	10
Dynamic	35–90	Distilled water	3–1,200 cm^3/hr	Grains or monoliths	11
Grain Titration	100	Distilled water	Static	Powder	12
Time-Dependent Method	20– ~60	Buffered water	Static	Disc	10
MCC–1	40, 70, 90	Distilled water and reference groundwater	Static	Monolith SA/V = 10 m^{-1}	4

Table 1. Summary of leach test methods[6] (cont'd)

Name of Test	Temperature (°C)	Leachant	Flow Rate	Sample Description	Reference
MCC–2	110, 150, 190	Distilled water and reference groundwater	Static	Monolith SA/V = 10 m^{-1}	4
MCC–3	40, 90, 110, 150, 190	Distilled water and reference groundwater	Static (agitated)	Crushed (1) 149–175 μm (2) <45 μm	4
HTLT (CEC)	90, 110 150, 190	Distilled water	Static	SA = 4 cm^2	13
Autoclave (HMI)	150–200	Distilled water and brines	Static	Beads, chips	14
Autoclave (KfK)	100, 150, 200, 250	Distilled water and brines	Static	Cylinders SA = 20 or 5 cm^2	15
Repository Simulation	25–90	Granite equilibrated water	None (sampling equivalent to 1 cm^3/mo)	Plate SA = 3 cm^2	10
Waste/Water/ Rock Leach	98	Distilled water or granite water		Glass cube: SA = 6 cm^2 20 g granite powder: 250–710 μm, 60 cm^2 water	5
MCC–14	25–250	Repository groundwaters	Static or periodic sampling	Monoliths and powders	4
PCT	90	Deionized water	Static	Crushed 74–149 μm	16

1 Nakamura H., and S. Toshiro. *Safety Research of High-Level Waste Management for the Period April 1982 to March 1983.* Progress Report JAERI–M–83–076. Japan Atomic Energy Research Institute. 1983.

2 Hussain, M., and L. Kahl. Incorporation of precipitation from treatment of medium-level liquid radioactive waste in glass matrix or ceramics together with high-level waste. *Symposium Proceedings for the Ceramic in Nuclear Waste Management.* 1979.

3 Commission of the European Communities. *Testing and Evaluation of Solidified High-Level Waste Forms.* Joint Annual Progress Report EUR 10038. Commission of European Communities (CEC). 1983.

4 U.S. Department of Energy. *Nuclear Waste Material Handbook (Test Methods) Technical Information Center.* DOE/TIC–11400. Washington, DC: U.S. Department of Energy. 1981.

5 Igarashi, H. et al. Leaching test of simulated HLW glass in the presence of rock. *Atomic Energy Society of Japan—1983 Annual Meeting.* 1983.

6 Senoo, M. et al. *High-Pressure Soxhlet-Type Leachability Testing Device and Leaching Test of Simulated High-Level Waste Glass at High Temperature.* JAERI–M–8571. Japan Atomic Energy Research Institute. 1979.

7 Draft International Standard Report. ISO/DIS–6961. 1979.

Table 1. Summary of leach test methods[6] (cont'd)

Name of Test	Temperature (°C)	Leachant	Flow Rate	Sample Description	Reference

8 Oversby, V.M., and A.E. Ringwood. Leaching studies on Synroc at 95 and 200 °C. *Radioactive Waste Management* 23: 223. 1982.

9 Reeve, K.D., et al. The development of testing of Synroc for high-level radioactive waste fixation. *Symposium Proceedings for the Waste Management* 1: 249–266. 1981.

10 Van Iseghem, P., et al. Chemical Stability of Simulated HLW Forms in Contact with Clay Media. EUR–8424. CCC. 1983.

11 Vaswani, G.A., et al. Development of Improved Leaching Techniques for Vitrified Radioactive Waste Products. BARC–1032. Bhabba Atomic Research Center. 1978.

12 Deutsches Institut for Normung. *DIN Leach Test.* Report 12111. Deutsches Institut for Normung. 1976.

13 European Community Static High Temperature Test Summary. CEC Report EUR 9772. 1985.

14 Altenhein, F.K., et al. Scientific Basic International Symposium Proceedings for the Nuclear Waste Management: 363–370. 1981.

15 Kahl, L., M.C. Ruiz-Lopez, J. Saidl, and T. Dippl. Preparation and Characterization of an Improved Borosilicate Glass for Solidification of High-Level Radioactive Fission Product Solutions. Part 2: Characterization of the Borosilicate Glass Product. GP 98/12. Kernforschungszentrum Karlsruhe Report KFK–3251e. 1982.

16 American Society for Testing and Materials. *Determining Chemical Durability of Nuclear, Hazardous, and Mixed Waste Glasses: The Product Consistency Test.* Annual Book of ASTM Standards. ASTM C 1285-97. Volume 12.01. 774–91. West Conshohocken, PA: American Society for Testing and Materials. 1997.

Table 2. Leaching experimental results after varying composition[6]

Composition Change	Durability	Glass Composition	Reference
(Ca, Mg, Zn) for Si	Increases	Simple glass	1
(Mg, Ca) for Si	Increases	Simple glass	2
Ca for Si	Increases	Simple glass	3
(Sr, Ba) for Si	Decreases	Simple glass	2
(Na, K, Li) for Si	Decreases	Simple glass	4
Na for Si	Negligible	Waste glass	5
Al for Si	Increases	Simple glass	6
Ca for (Na, K)	Decreases	Waste glass	5
Na for Al	Negligible	Waste glass	5
Na for K	Variable	Mixed alkali effect	7
Na for K	Negligible	No mixed alkali effect	5
Al for Fe	Increases	Waste glass	8
Fe^{3+} for Zn	Decreases	Waste glass	9
Increase (Si, Al, Zr)	Increases	Waste glass	10, 11
Increase Al	Increases	Waste glass	12
Increase (Al, Cr, Si)	Increases	Waste glass, MCC–1 tests	13
Increase Al	Decreases	Waste glass, acid leachate	13
Increase B	Decreases	Waste glass	13
Increase B	Increases	Waste glass	10
Increase (Na, Li)	Decreases	Waste glass	14
Increase Alkali	Decreases	Waste glass	10, 11
Increase (Na, Ca)	Decreases	Waste glass, MCC–1 tests	13
Increase (Mg, Ca)	Negligible	Waste glass	10
Increase Ti	Variable	Waste glass	11
Increase Ti	Increases	Waste glass	13

Table 2. Leaching experimental results after varying composition[6] (cont'd)

Composition Change	Durability	Glass Composition	Reference
Increase (Cu, Cr, Ni)	Negligible	Waste glass	11
Increase La	Increases	Waste glass	11
Increase Zn	Decreases	Waste glass, MCC–1 tests	13
Increase Zn	Decreases	Waste glass	11
Fe^{3+} for Fe^{2+}	Increases	Waste glass	10
Fe^{3+} for Fe^{2+}	Negligible	Waste glass	8

1 Smets, B.M., M.G.W. Tholen, and T.P.A. Lommen. The effect of divalent cations on the leaching kinetics of glass. *J. Non-Crys. Sol.* 65: 319–332. 1984.

2 Isard, J.O., and W. Muller. Influence of alkaline earth ions on the corrosion of glasses. *Phys. Chem. Glasses* 27(2): 55–58. 1986.

3 Rana, M.A., and R.W. Douglas. The reaction between glass and water—Part I: Experimental methods and observations. *Phys. Chem. Glasses* 2(6): 179–195. 1961a.
Rana, M.A., and R.W. Douglas. The reaction between glass and water—Part 2: Discussion of the results. *Phys. Chem. Glasses* 2(6): 196–204. 1961b.

4 Douglas, R.W., and T.M.M. El-Shamy. Reactions of glasses with aqueous solutions. *J. Am. Ceram. Soc.* 50(1): 1–8. 1967.

5 Tait, J., and D.L. Mandelosi. *The Chemical Durability of Alkali Aluminosilicate Glasses.* Atomic Energy of Canada Limited Report AECL–7803. Pinawa Manitoba, Canada: Atomic Energy of Canada Limited. 1983.

6 Smets, B.M.J., and T.P.A. Lommen. The leaching of sodium aluminosilicate glasses studied by secondary ion mass spectrometry. *Phys. Chem. Glasses* 23(3): 83–87. 1982.

7 Dilmore, M.F., D.E. Clark, and L.L. Hench. Chemical durability of Na_2O-K_2O-CaO-SiO_2 glasses. *J. Am. Ceram. Soc.* 61: 439–443. 1978.

8 Van Iseghem, P., and R. de Batist. Corrosion mechanisms of simulated high level nuclear waste glasses in distilled water. *Riv. Della Staz. Sper. Vetro* 5: 163–170. 1984.

9 Nogues, J.L., and L.L. Hench. Effect of Fe_2O_3/ZnO on two glass compositions for solidification of Swedish nuclear wastes. *Proceedings of the Materials Research Society Symposium.* Symposium Proceedings 11. Pittsburgh, PA: Materials Research Society: 273–278. 1982.

10 Feng, X., I.L. Pegg, Y. Guo, Aa. Barkatt, P.B. Macedo, S.J. Cucinell, and S. Lai. Correlation between composition effects on glass durability and the structural role of the constituent oxides. *Nucl. Technol.* 85: 334–345. 1989.

11 Macedo, P.B., S.M. Finger, A.A. Barkatt, I.L. Pegg, X. Feng, and W.P. Freeborn. *Durability Testing with West Valley Borosilicate Glass Composition—Phase II.* West Valley Nuclear Services Topical Report DOE/NE/44139-48. West Valley, NY: West Valley Nuclear Services, Inc.. 1988.

12 Nogues, J.L., L.L. Hench, and J. Zarzycki. Comparative study of seven glasses for solidification of nuclear wastes. *Proceedings of the Materials Research Society Symposium.* Symposium Proceedings: 11. Pittsburgh, PA: Materials Research Society: 211–218. 1982.

13 Chick, L.A., G.F. Piepel, G.B. Mellinger, R.P. May, W.J. Gray, and C.Q. Buckwalter. *The Effects of Composition on Properties in an 11-Component Nuclear Waste Glass System.* Pacific Northwest Laboratory Report PNL–3188. Richland, WA: Pacific Northwest National Laboratory. 1981.

14 Diebold, F.E., and J.K. Bates. Glass-water vapor interaction. *Adv. in Ceram.* 20: 515–522. 1986.

Table 3. Primary basis set of partial molar hydration free energies, ΔG_i, for glass in oxidized pH regimes >7[41]

Hydration Reactions	ΔG_i kcal/mole	pH Range
$Al_2O_3 + H_2O \rightarrow 2AlO_2^-{}_{(aq)} + 2H^+{}_{(aq)}$	+37.68	7–14
$AmO_2 + 3H_2O \rightarrow Am(OH)_5^-{}_{(aq)} + H^+{}_{(aq)}$	+23.68	7–14
$As_2O_3 + 3H_2O + O_2 \rightarrow 2HAsO_4^{-2}{}_{(aq)} + 4H^+{}_{(aq)}$	-33.65	7–11
$B_2O_3 + 3H_2O \rightarrow 3H_3BO_{3(aq)}$	-10.43	7–10
$\{BaO + SiO_2\} + 2H_2O \rightarrow Ba(OH)_2 + H_2SiO_{3(aq)}$	-19.13	7–14
$\{CaO + SiO_2\} + 2H_2O \rightarrow Ca(OH)_2 + H_2SiO_{3(aq)}$	-9.74	7–14
$\{CdO + SiO_2\} + 2H_2O \rightarrow Cd(OH)_2 + H_2SiO_{3(aq)}$	+2.31	7–14
$Ce_2O_3 + 3H_2O \rightarrow 2Ce(OH)_3$	-44.99	7–14
$\{CoO + SiO_2\} + \frac{5}{2}H_2O + \frac{1}{4}O_2 \rightarrow Co(OH)_3 + H_2SiO_{3(aq)}$	-2.33	7–14
$Cr_2O_3 + 3H_2O \rightarrow 2Cr(OH)_3$	+11.95	7–14
$\{Cs_2O + SiO_2\} + 2H_2O \rightarrow 2Cs^+{}_{(aq)} + 2OH^-{}_{(aq)} + H_2SiO_{3(aq)}$	-76.33	7–14
$\{Cu_2O + SiO_2\} + \frac{1}{2}O_2 + 3H_2O \rightarrow 2Cu(OH)_2 + H_2SiO_{3(aq)}$	-18.85	7–14
$\{CuO + SiO_2\} + 2H_2O \rightarrow Cu(OH)_2 + H_2SiO_{3(aq)}$	+5.59	7–14
$\{FeO + SiO_2\} + \frac{1}{4}O_2 + \frac{5}{2}H_2O \rightarrow Fe(OH)_3 + H_2SiO_{3(aq)}$	-17.28	7–14
$Fe_2O_3 + 3H_2O \rightarrow 2Fe(OH)_3$	+14.56	7–14
$\{K_2O + SiO_2\} + 2H_2O \rightarrow 2K^+{}_{(aq)} + 2OH^-{}_{(aq)} + H_2SiO_{3(aq)}$	-72.36	7–14
$La_2O_3 + 3H_2O \rightarrow 2La(OH)_3$	-48.59	7–14
$\{Li_2O + SiO_2\} + 2H_2O \rightarrow 2Li^+{}_{(aq)} + 2OH^-{}_{(aq)} + H_2SiO_{3(aq)}$	-19.99	7–14
$\{MgO + SiO_2\} + 2H_2O \rightarrow Mg(OH)_2 + H_2SiO_{3(aq)}$	-2.52	7–14
$\{MnO + SiO_2\} + \frac{1}{2}O_2 + H_2O \rightarrow MnO_2 + H_2SiO_{3(aq)}$	-20.39	7–14
$MoO_3 + H_2O \rightarrow 2H^+{}_{(aq)} + MoO_4^{-2}{}_{(aq)}$	+16.46	7–14

48/85

Table 3. Primary basis set of partial molar hydration free energies, ΔG_i, for glass in oxidized pH regimes >7[41]

Hydration Reactions	ΔG_i kcal/mole	pH Range
$\{Na_2O + SiO_2\} + 2H_2O \rightarrow 2Na^+_{(aq)} + 2OH^-_{(aq)} + H_2SiO_{3(aq)}$	-49.04	7–14
$Nd_2O_3 + 3H_2O \rightarrow 2Nd(OH)_3$	-37.79	7–14
$\{NiO + SiO_2\} + 2H_2O \rightarrow Ni(OH)_2 + H_2SiO_{3(aq)}$	+4.42	7–14
$P_2O_5 + 3H_2O \rightarrow 2HPO_4^{-2}{}_{(aq)} + 4H^+_{(aq)}$	-26.55	7–12
$\{PbO + SiO_2\} + 2H_2O \rightarrow HPbO_2^-{}_{(aq)} + H_2SiO_{3(aq)} + H^+_{(aq)}$	+25.10	7–14
$PuO_2 + 3H_2O \rightarrow Pu(OH)_5^-{}_{(aq)} + H^+_{(aq)}$	+30.75	7–14
$\{Rb_2O + SiO_2\} + 2H_2O \rightarrow 2Rb^+_{(aq)} + 2OH^-_{(aq)} + H_2SiO_{3(aq)}$	-82.18	7–14
$RuO_2 + \frac{1}{2} O_2 + H_2O \rightarrow RuO_4^-{}_{(aq)} + 2H^+_{(aq)}$	+57.30	7–10
$Sb_2O_3 + O_2 + H_2O \rightarrow 2SbO_3^-{}_{(aq)} + 2H^+_{(aq)}$	-37.56	7–14
$SeO_2 + \frac{1}{2} O_2 + H_2O \rightarrow SeO_4^{-2}{}_{(aq)} + 2H^+_{(aq)}$	-7.80	7–14
$SiO_2\ H_2O \rightarrow H_2SiO_{3(aq)}$	+4.05	7–10
$SnO_2 + 2H_2O \rightarrow Sn(OH)_4$	+10.16	7–12
$\{SrO + SiO_2\} + 2H_2O \rightarrow Sr(OH)_2 + H_2SiO_{3(aq)}$	-15.16	7–14
$TcO_2 + \frac{1}{2} O_2 + H_2O \rightarrow TcO_4^-{}_{(aq)} + 2H^+_{(aq)}$	-2.04	7–14
$TeO_2 + \frac{1}{2} O_2 + H_2O \rightarrow TeO_4^{-2}{}_{(aq)} + 2H^+_{(aq)}$	+12.02	7–14
$ThO_2 + H_2O \rightarrow Th(OH)_4$	+19.23	7–14

Table 4. Composition region (mass fraction) studied by Hrma[42]

	HW–39–4	Lower Limit	Upper Limit
SiO_2	0.5353	0.42	0.57
B_2O_3	0.1053	0.05	0.20
Na_2O	0.1125	0.05	0.20
Li_2O	0.0375	0.01	0.07
CaO	0.0083	0.00	0.10
MgO	0.0084	0.00	0.08
Fe_2O_3	0.0719	0.02	0.15
Al_2O_3	0.0231	0.00	0.15
ZrO_2	0.0385	0.00	0.13
Others	0.0592	0.01	0.10

Table 5. Regression coefficients for normalized release and pH using 28-d MCC–1 method[42]

x_i	b_i (Si)	b_i (B)	b_i (Li)	b_i (Na)	b_i (pH)
SiO_2	0.9025	-0.0993	-0.2319	-0.0587	7.3144
B_2O_3	6.8360	9.6800	9.4346	9.6671	9.1180
Na_2O	7.1851	9.5454	9.1998	8.9623	17.8061
Li_2O	9.6783	11.8108	10.5425	12.2173	24.4490
CaO	2.0185	3.7572	4.7685	3.6144	13.3174
MgO	1.8500	5.1079	4.9844	5.0078	13.1459
Fe_2O_3	4.6516	5.7008	6.0434	5.7557	10.1817
Al_2O_3	-4.6186	-6.2911	-5.6794	-6.0434	4.0454
ZrO_2	-2.1819	-0.6283	-0.2328	-0.7562	7.5917
Others	1.9548	3.6529	4.1125	3.4126	8.6750
# points	114	114	114	114	120
r^2	0.5996	0.6520	0.6525	0.6532	0.7487

Table 6. Regression coefficients for normalized release and pH using the 7-d product consistency test method[42]

x_i	b_i (Si)	b_i (B)	b_i (Li)	b_i (Na)	b_i (pH)
SiO_2	-2.9671	-4.3173	-3.2278	-4.4118	8.1926
B_2O_3	-0.6148	11.9791	10.1496	9.4049	3.3332
Na_2O	10.7384	17.6068	14.0017	19.4013	23.6171
Li_2O	19.7370	22.5791	18.4159	19.0635	31.2448
CaO	-6.0415	-8.7114	-5.3528	-1.9567	17.2056
MgO	2.9296	10.9210	7.1181	11.8228	15.3354
Fe_2O_3	-4.2315	-3.2009	-4.5113	-4.0953	8.5939
Al_2O_3	-17.3377	-25.4071	-22.3095	-25.4294	5.3578
ZrO_2	-10.8139	-10.5613	-10.0618	-11.4209	7.6111
Others	-0.7297	0.1587	0.6181	0.6647	9.2689
# points	123	123	123	123	123
r^2	0.7377	0.8114	0.7905	0.8457	0.9092

52/89

Fig. 1. Effect of pH on the rate of extraction of silica from fused silica powder at 80 °C[8]

53/85

Fig. 2. Effect of pH on the extraction of soda and silica from a $Na_2O{\cdot}3SiO_2$ glass at 35 ° C[8]

54/89

Fig. 3. Schematic of surface layers on leached glass

55/69

Fig. 4. Concentration versus (SA/V)•time for release of B from SRL–131 at 90 °C at (●) 10, (■) 2,000, and (◆) 20,000 m^{-1} [16]

56/85

Fig. 5. Leachate pH values (25 °C) versus reaction time for SRL–131 glass and glass reacted at 90 °C at (●) 10, (■) 2,000, and (◆) 20,000 m^{-1} [16]

57/85

Fig. 6. Normalized release rates of sodium and silicon as a function of leachant flow rates[18]

Fig. 7. Normalized total mass loss versus leach time for various flow rates[19]

Fig. 8. Normalized elemental mass loss versus temperature for different leaching durations[20]

60/87

Fig. 9. Summary diagram indicating reported activation energies for individual reaction processes and overall activation energies for high-level waste glass studies[6]

61/85

Fig. 10. Leaching (MCC–3 test, 90 °C) of WV–205 glass as a function of glass redox state[29]

62/89

Fig. 11. Interpolated surface showing the dependence of MCC–3 boron concentration on test time and amount of SiO_2 added to WV–205[30]

63/89

Fig. 12. Interpolated surface showing the dependence of MCC–3 boron concentration on test time and amount of ZrO_2 added to WV–205[30]

Fig. 13. Interpolated surface showing the dependence of MCC–3 boron concentration on test time and amount of Al_2O_3 added to WV–205[30]

Fig. 14. The Si leach rates ($mg/m^2/d$) of glass WV–205 in deionized water, 0.1 M KNO_3, 0.1 M $Ba(NO_3)_2$ and 0.1 M $CsNO_3$ solutions at neutral pH for up to 200 d of leaching

64/89

Fig. 15. Cumulative normalized leach concentration for boron versus time for the West Valley Demonstration Project (WVDP) glass in various solutions[40]

67/85

Fig. 16. Normalized leach rate for various elements versus leachate pH after the first solution replacement for West Valley Demonstration Project (WVDP) glass[40]

Fig. 17. (a) Linear regression plots of the ΔG_{hyd} term versus silicon release to the leachant in a 28-day static leach test. The ΔG_{hyd} term has been adjusted for pH changes, as discussed in the text. (b) Linear regression plots of the ΔG_{hyd} term versus boron release to the leachant in a 28-day static leach test. The ΔG_{hyd} term has been adjusted for pH changes, as discussed in the text.[3]

Fig. 18. Predicted component effects on MCC–1 release relative to the HW–39–4 composition, based on the first-order mixture model using mass fractions fitted to the reduced data set[42]

Fig. 19. Predicted component effects on PCT B release relative to the HW–39–4 composition, based on the first-order mixture model using mass fractions[42]

Fig. 1 71/85

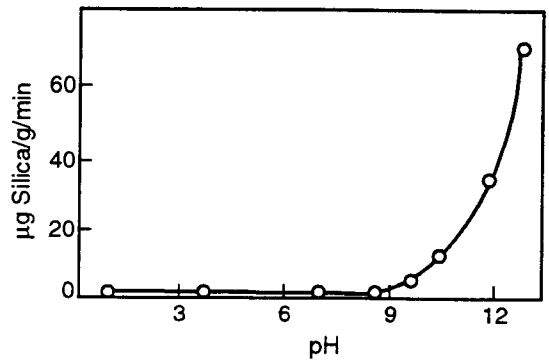

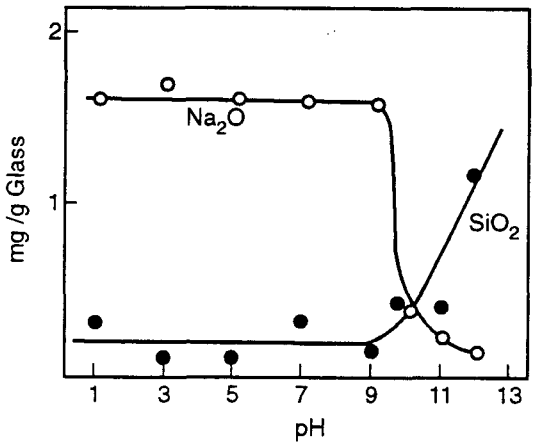
2
1
mg /g Glass
Na_2O
SiO_2
1
3
5
7
9
11
13
pH

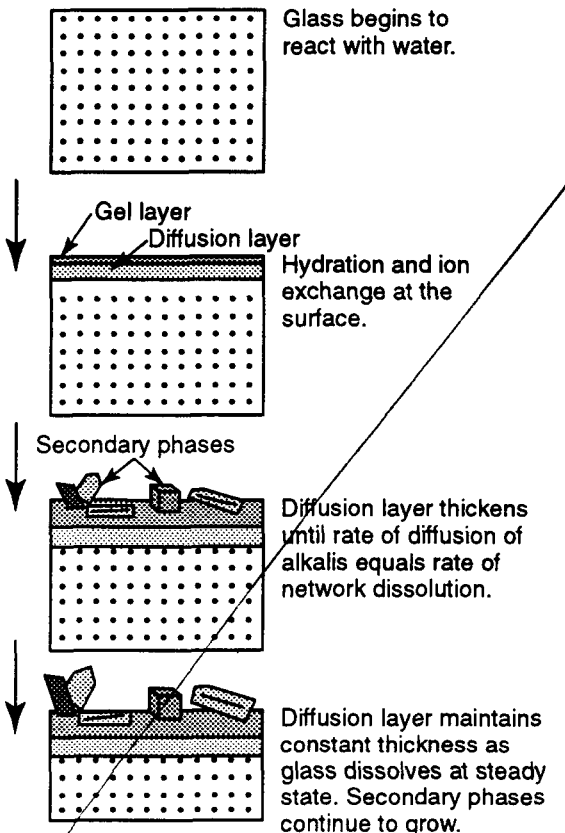
Glass begins to react with water.
Gel layer
Diffusion layer
Hydration and ion exchange at the surface.
Secondary phases
Diffusion layer thickens until rate of diffusion of alkalis equals rate of network dissolution.
Diffusion layer maintains constant thickness as glass dissolves at steady state. Secondary phases continue to grow.

(a)

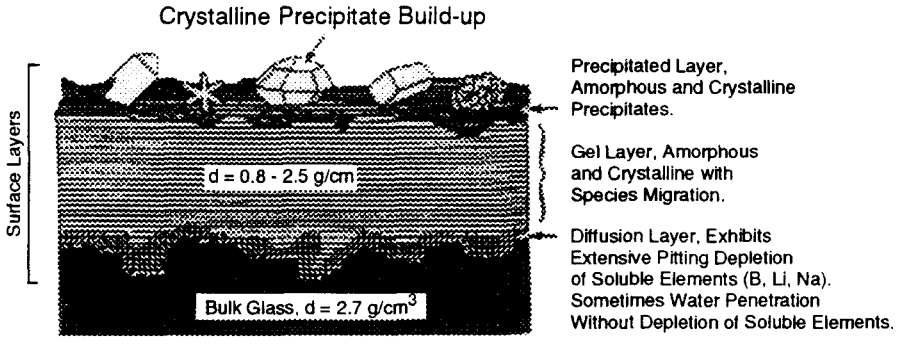
Crystalline Precipitate Build-up
Surface Layers
d = 0.8 - 2.5 g/cm
Bulk Glass, d = 2.7 g/cm3
Precipitated Layer, Amorphous and Crystalline Precipitates.
Gel Layer, Amorphous and Crystalline with Species Migration.
Diffusion Layer, Exhibits Extensive Pitting Depletion of Soluble Elements (B, Li, Na). Sometimes Water Penetration Without Depletion of Soluble Elements.

(b)

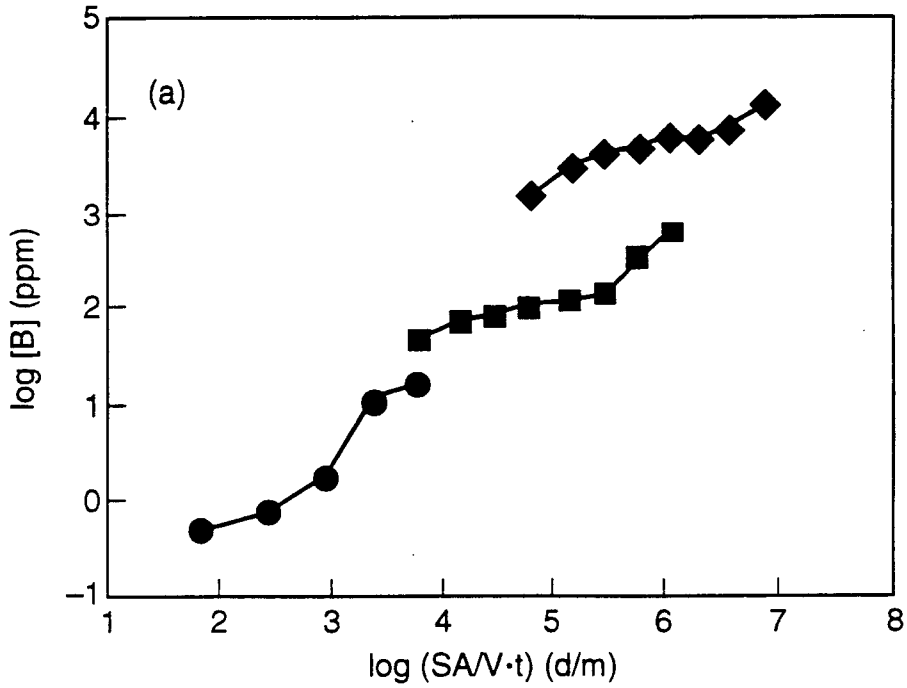
(a)
log [B] (ppm)
log (SA/V·t) (d/m)
5
4
3
2
1
0
−1
1
2
3
4
5
6
7
8

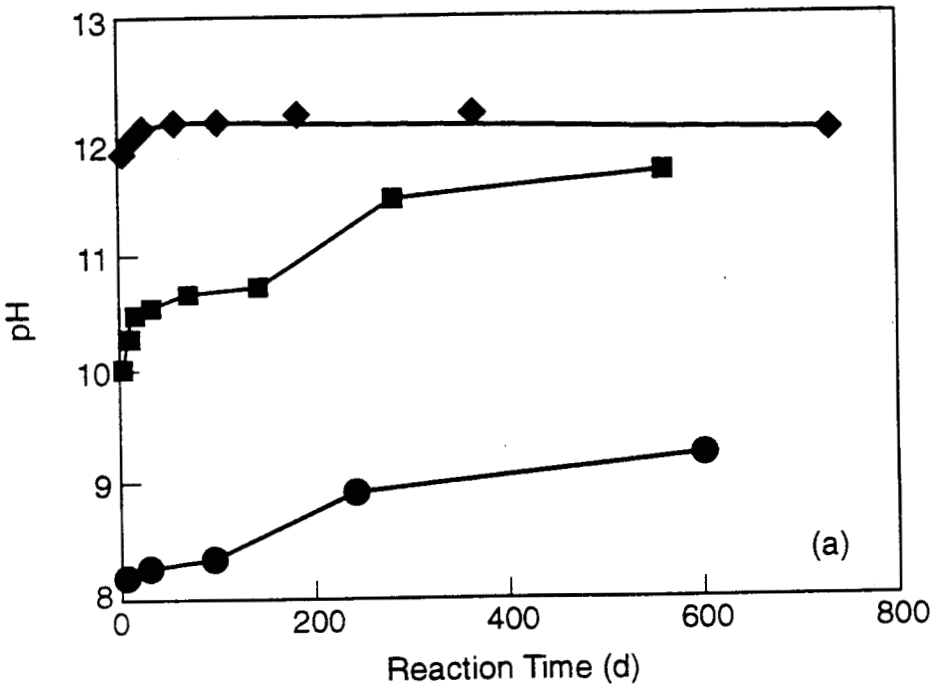
13
12
11
10
9
8
pH
0
200
400
600
800
Reaction Time (d)
(a)

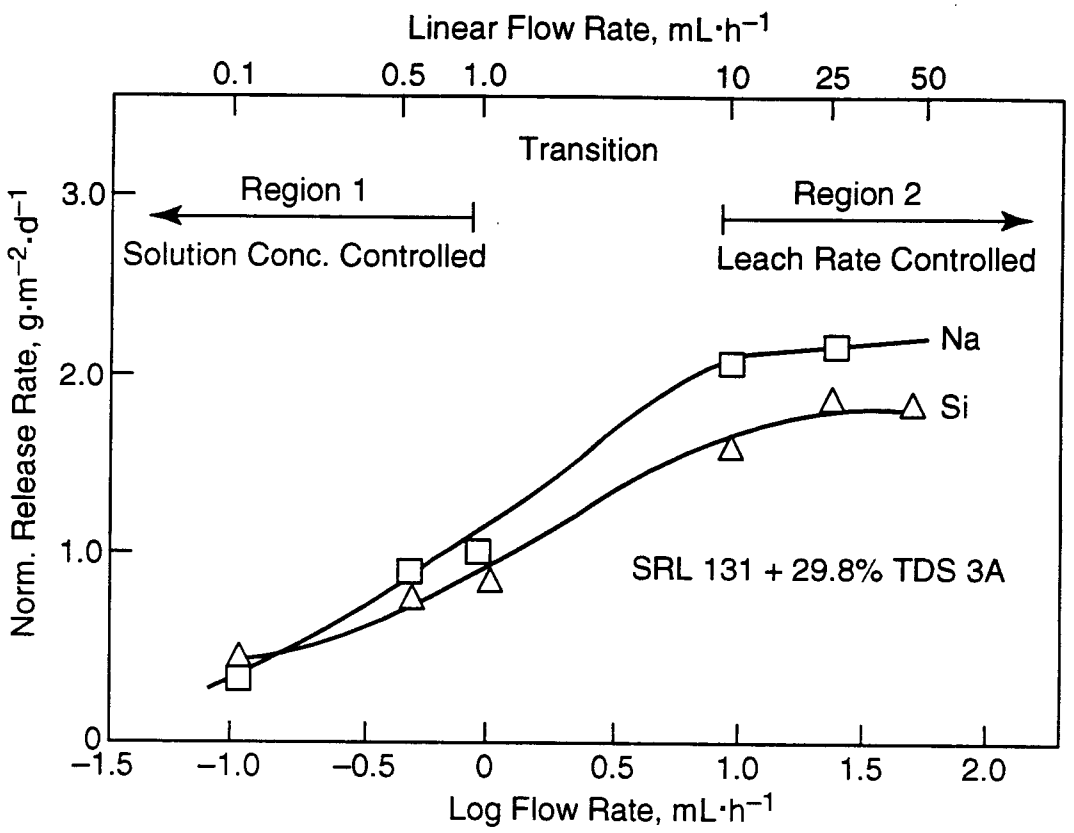
Linear Flow Rate, mL·h⁻¹
0.1
0.5
1.0
10
25
50
Transition
Region 1
Solution Conc. Controlled
Region 2
Leach Rate Controlled
Na
Si
SRL 131 + 29.8% TDS 3A
Norm. Release Rate, g·m⁻²·d⁻¹
3.0
2.0
1.0
0
−1.5
−1.0
−0.5
0
0.5
1.0
1.5
2.0
Log Flow Rate, mL·h⁻¹

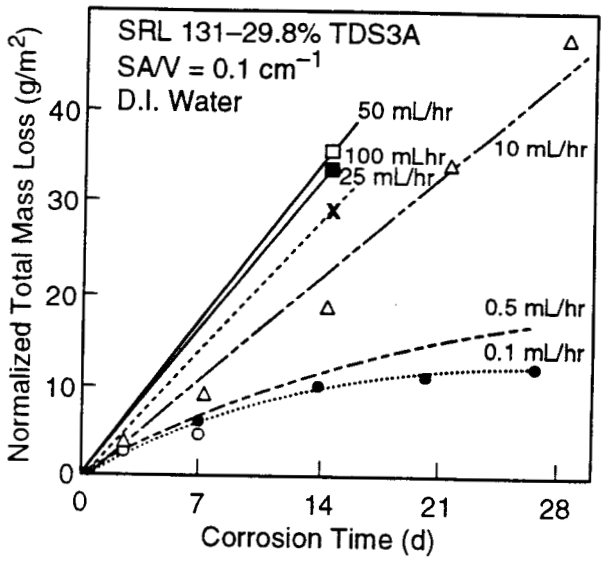
SRL 131–29.8% TDS3A
SA/V = 0.1 cm^{-1}
D.I. Water
50 mL/hr
100 mL/hr
25 mL/hr
10 mL/hr
0.5 mL/hr
0.1 mL/hr
Normalized Total Mass Loss (g/m^2)
0
10
20
30
40
0
7
14
21
28
Corrosion Time (d)

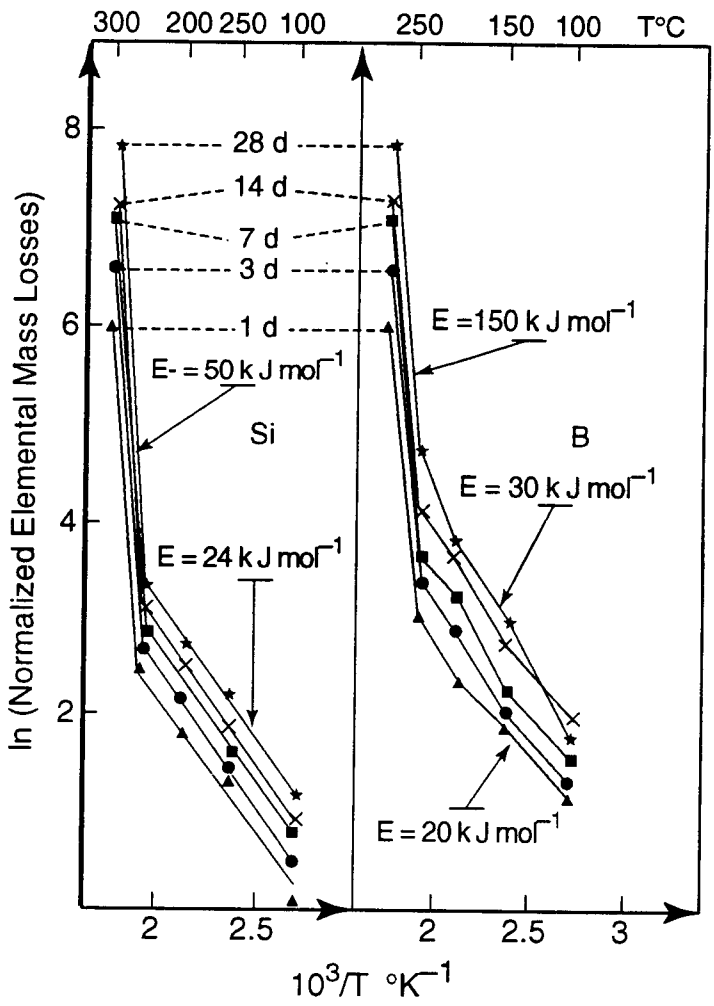
300 200 250 100
250 150 100 T°C
8
6
4
2
28 d
14 d
7 d
3 d
1 d
E- = 50 k J mol^{-1}
Si
E = 24 k J mol^{-1}
E =150 k J mol^{-1}
B
E = 30 k J mol^{-1}
E = 20 k J mol^{-1}
ln (Normalized Elemental Mass Losses)
2
2.5
2
2.5
3
$10^3/T$ °K^{-1}

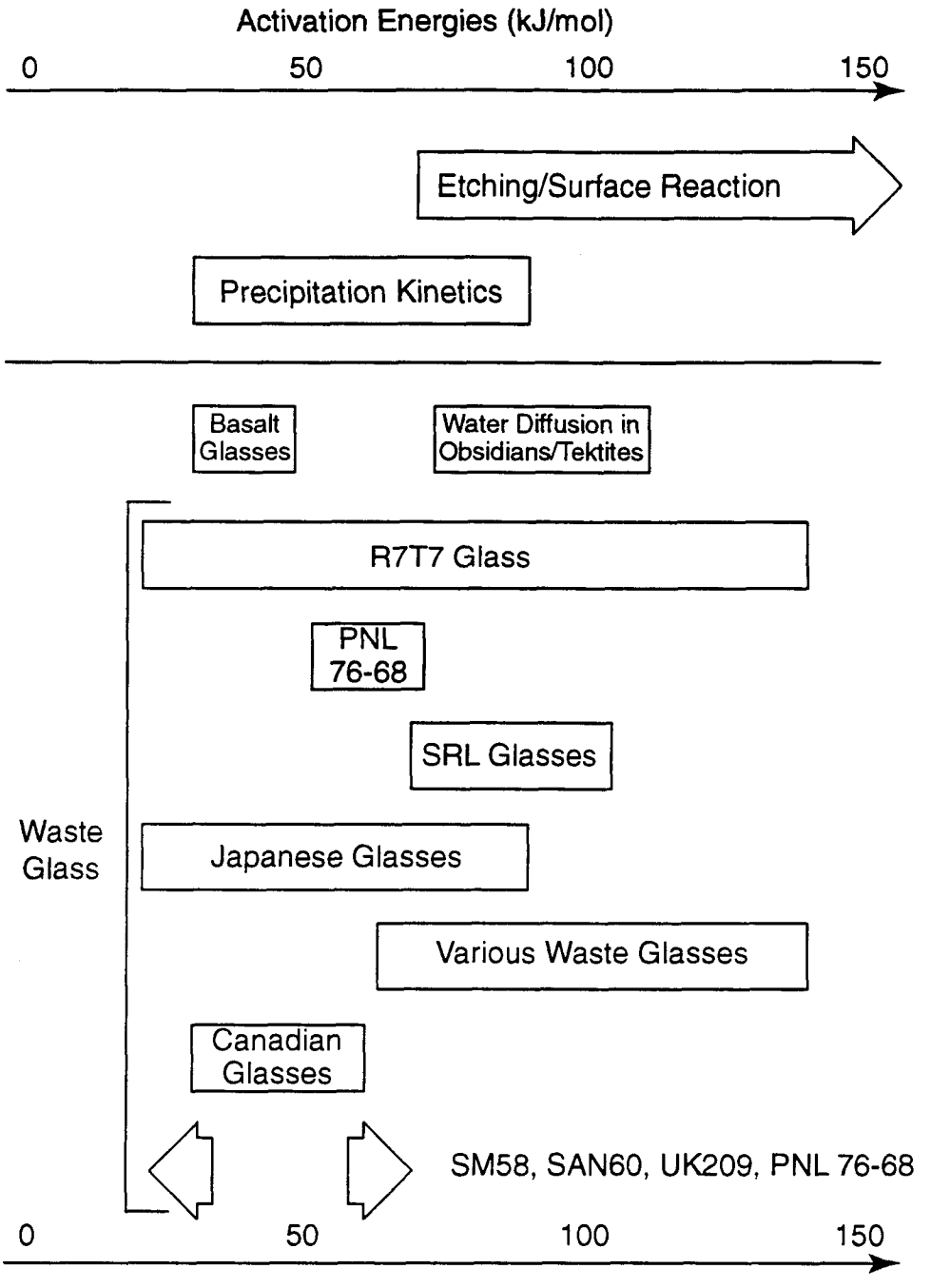
Activation Energies (kJ/mol)
0
50
100
150
Etching/Surface Reaction
Precipitation Kinetics
Basalt Glasses
Water Diffusion in Obsidians/Tektites
R7T7 Glass
PNL 76-68
SRL Glasses
Waste Glass
Japanese Glasses
Various Waste Glasses
Canadian Glasses
SM58, SAN60, UK209, PNL 76-68
0
50
100
150

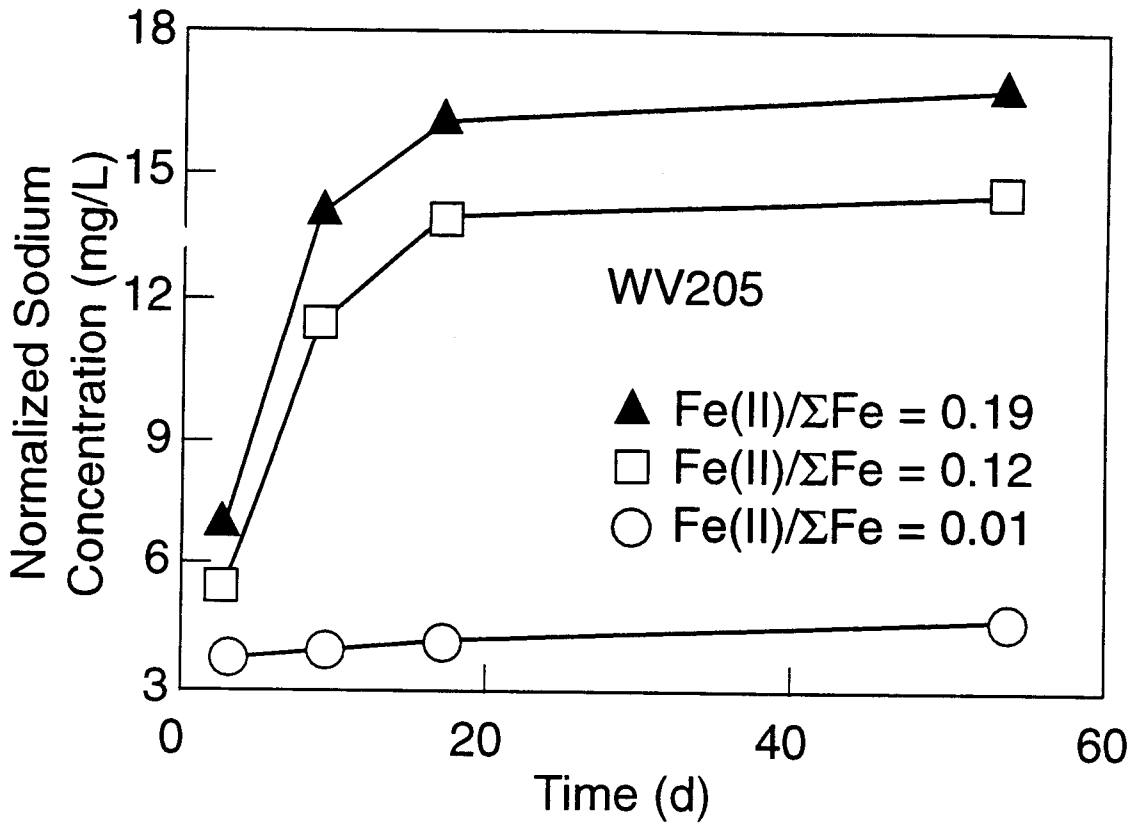
18
15
12
9
6
3
0
20
40
60
Normalized Sodium Concentration (mg/L)
Time (d)
WV205
▲ Fe(II)/ΣFe = 0.19
□ Fe(II)/ΣFe = 0.12
○ Fe(II)/ΣFe = 0.01

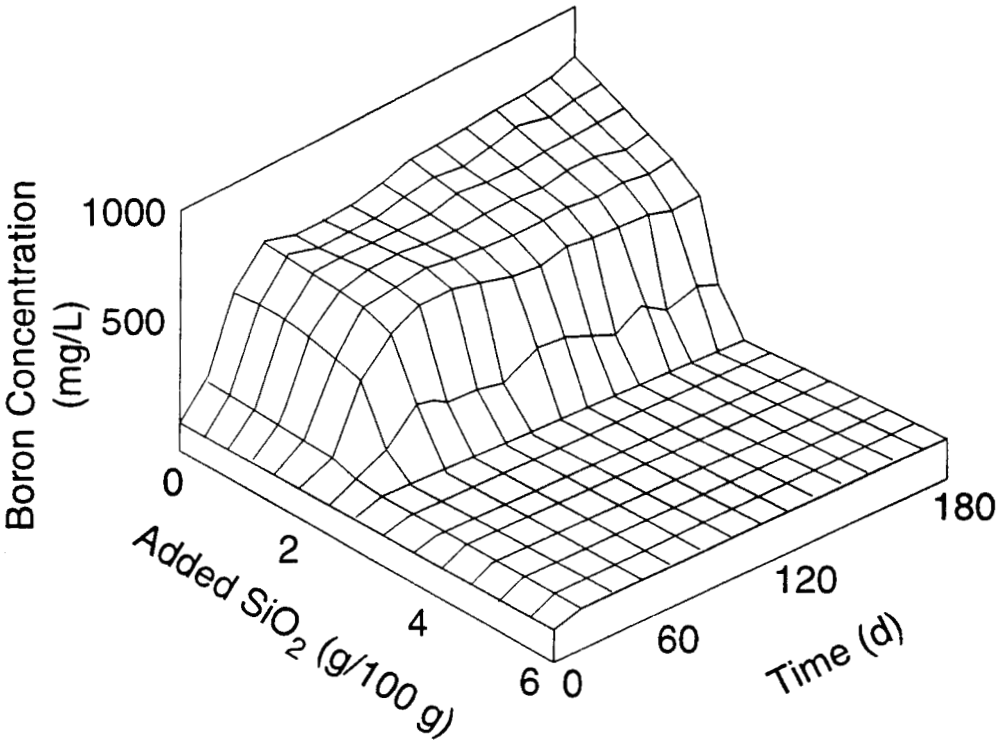
Boron Concentration
(mg/L)
1000
500
0
Added SiO_2 (g/100 g)
0
2
4
6
Time (d)
0
60
120
180

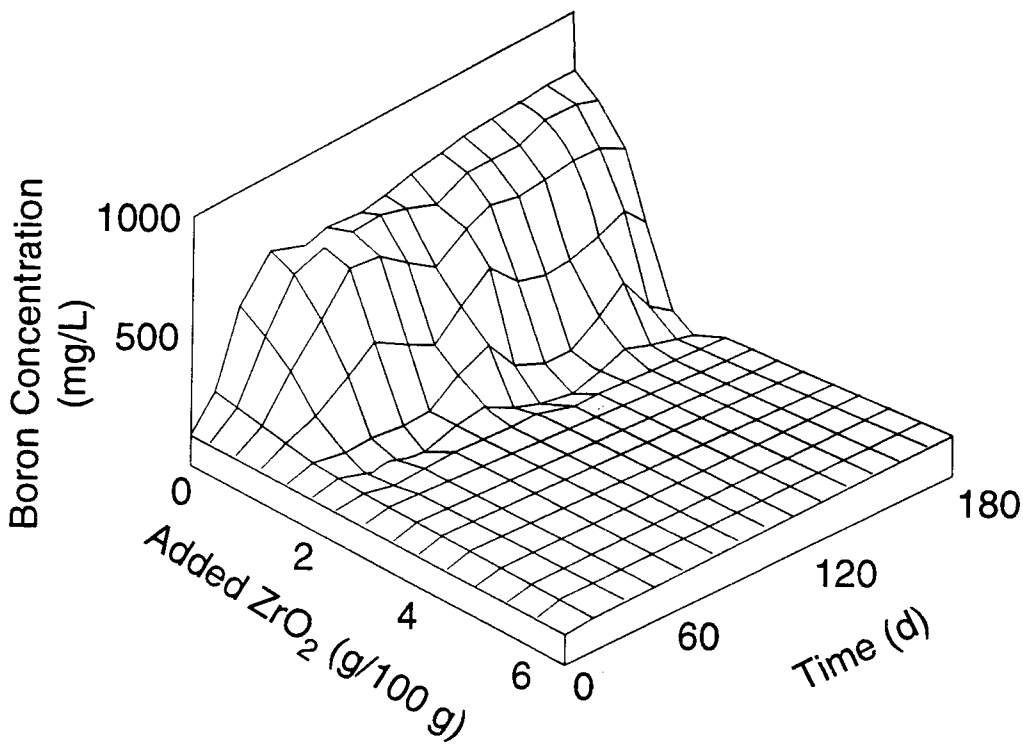
Boron Concentration (mg/L)
1000
500
0
Added ZrO_2 (g/100 g)
0
2
4
6
Time (d)
0
60
120
180

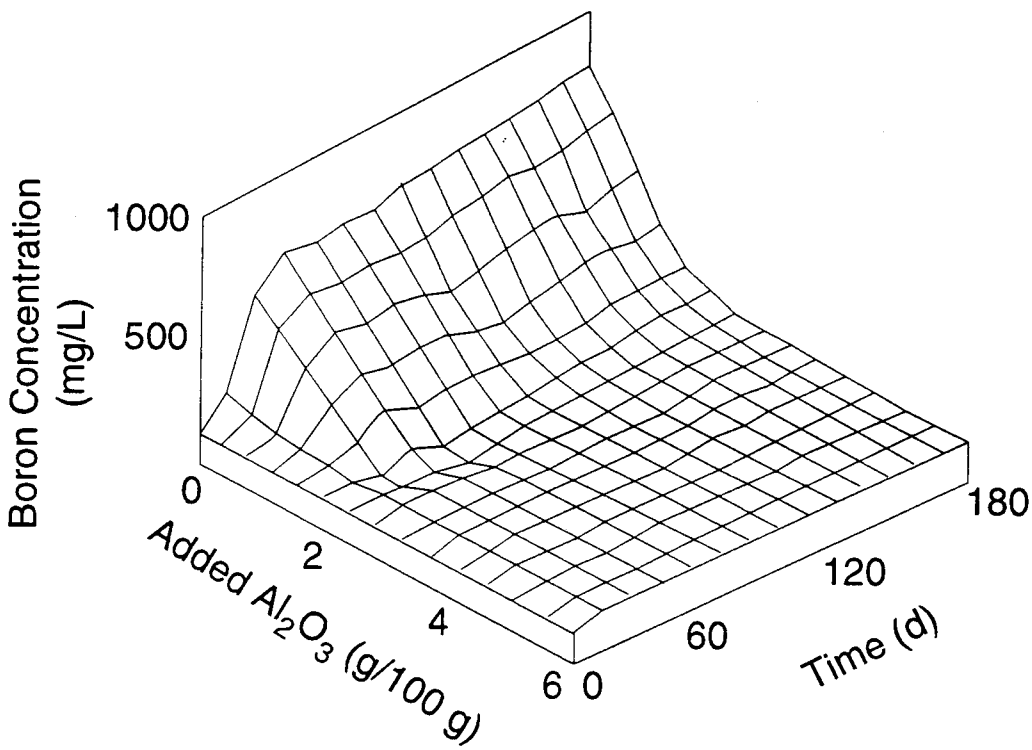
Boron Concentration (mg/L)
1000
500
0
Added Al_2O_3 (g/100 g)
0
2
4
6
Time (d)
0
60
120
180

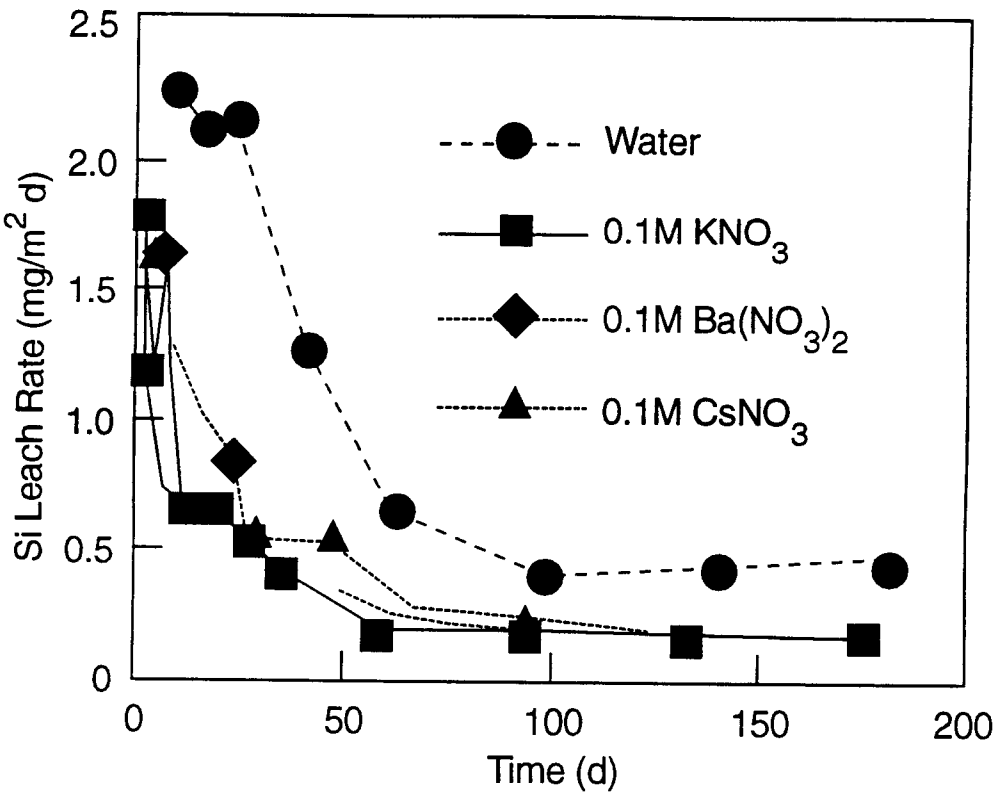
2.5
2.0
1.5
1.0
0.5
0
Si Leach Rate (mg/m^2 d)
0
50
100
150
200
Time (d)
Water
0.1M KNO$_3$
0.1M Ba(NO$_3$)$_2$
0.1M CsNO$_3$

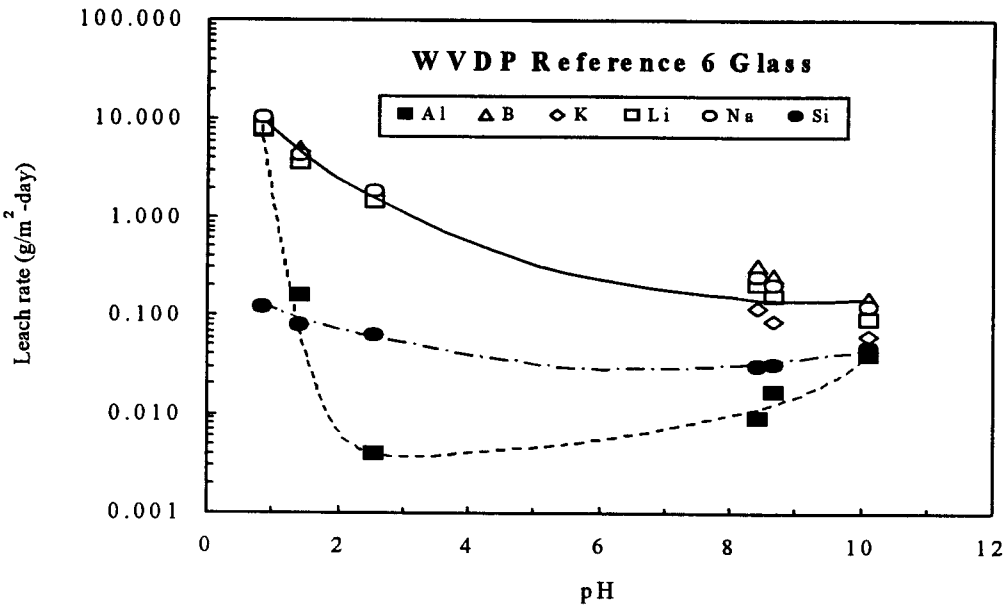
WVDP Reference 6 Glass
Al
B
K
Li
Na
Si
Leach rate (g/m2-day)
100.000
10.000
1.000
0.100
0.010
0.001
0
2
4
6
8
10
12
pH

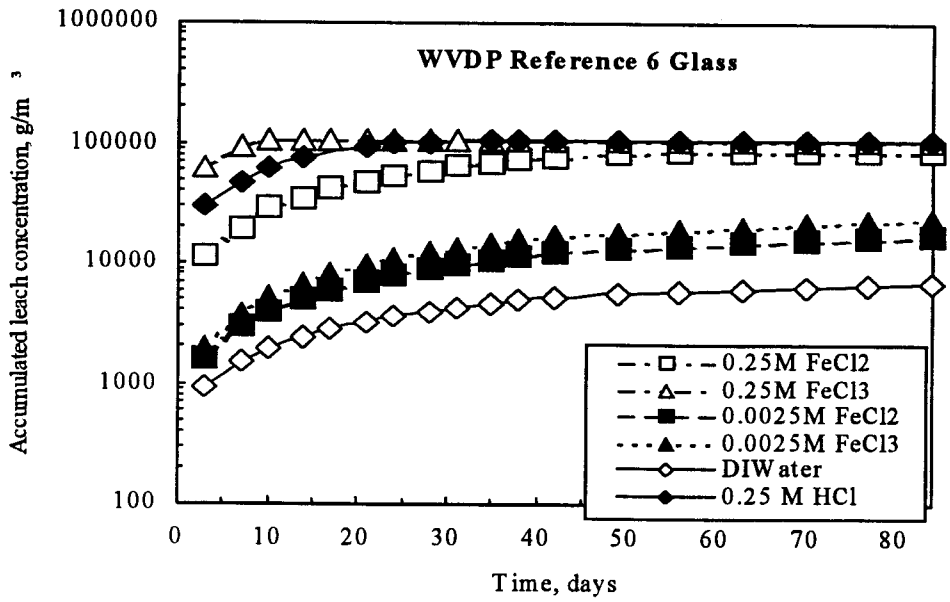
WVDP Reference 6 Glass
Accumulated leach concentration, g/m 3
1000000
100000
10000
1000
100
0
10
20
30
40
50
60
70
80
Time, days
0.25M FeCl2
0.25M FeCl3
0.0025M FeCl2
0.0025M FeCl3
DIWater
0.25 M HCl

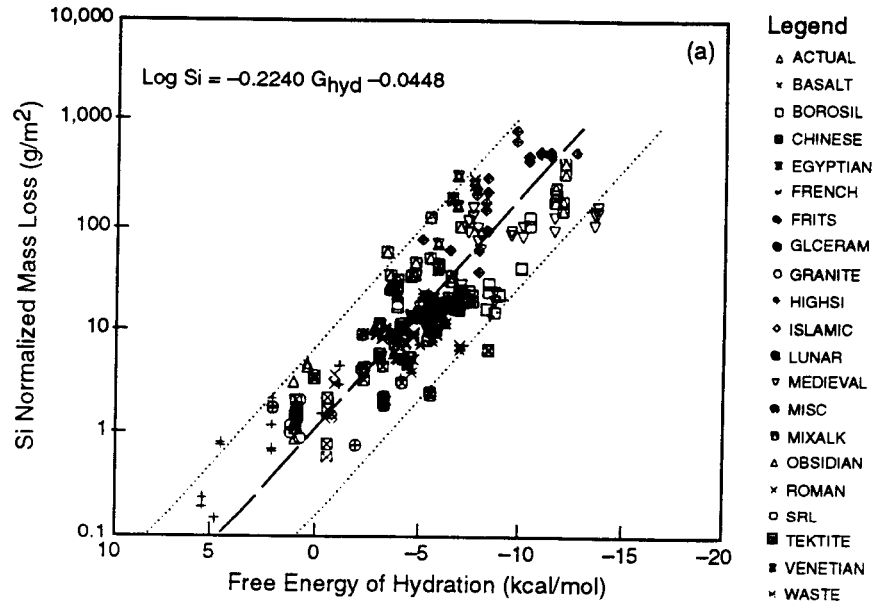
(a)
Log Si = −0.2240 G_{hyd} −0.0448
Si Normalized Mass Loss (g/m²)
10,000
1,000
100
10
1
0.1
10
5
0
−5
−10
−15
−20
Free Energy of Hydration (kcal/mol)
Legend
ACTUAL
BASALT
BOROSIL
CHINESE
EGYPTIAN
FRENCH
FRITS
GLCERAM
GRANITE
HIGHSI
ISLAMIC
LUNAR
MEDIEVAL
MISC
MIXALK
OBSIDIAN
ROMAN
SRL
TEKTITE
VENETIAN
WASTE

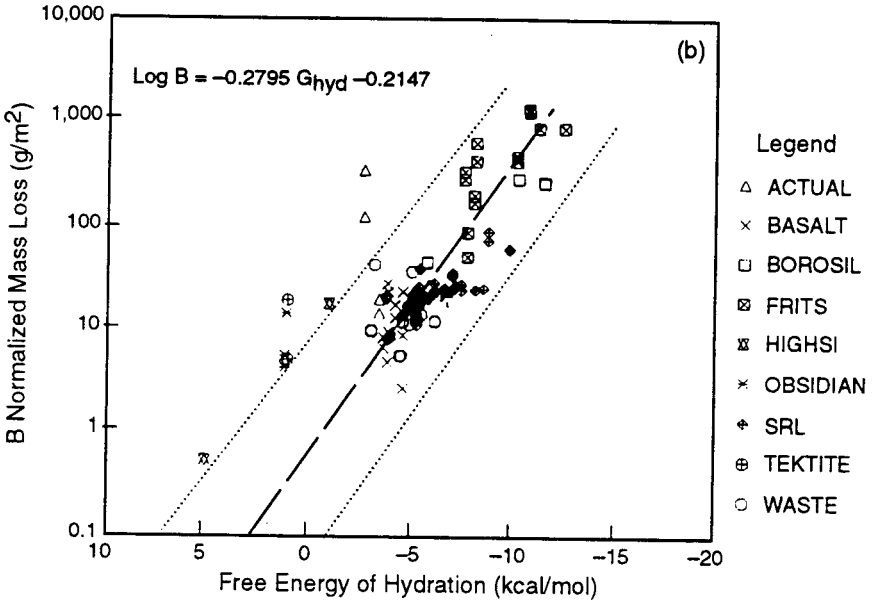
(b)
Log B = −0.2795 G_{hyd} −0.2147
B Normalized Mass Loss (g/m²)
10,000
1,000
100
10
1
0.1
10
5
0
−5
−10
−15
−20
Free Energy of Hydration (kcal/mol)
Legend
ACTUAL
BASALT
BOROSIL
FRITS
HIGHSI
OBSIDIAN
SRL
TEKTITE
WASTE

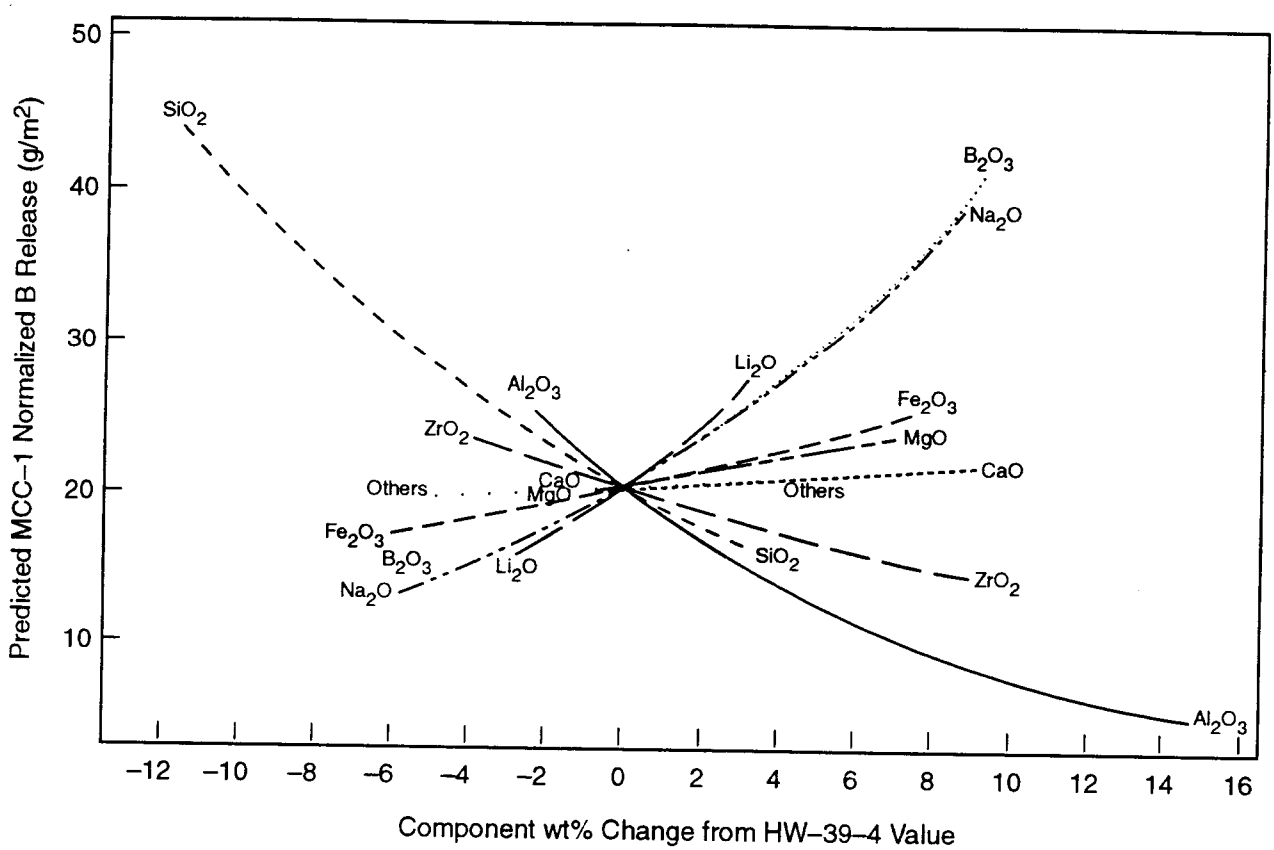
Predicted MCC–1 Normalized B Release (g/m²)
50
40
30
20
10
SiO2
B2O3
Na2O
Li2O
Al2O3
Fe2O3
ZrO2
MgO
CaO
Others
Others
Fe2O3
B2O3
Na2O
Li2O
SiO2
ZrO2
Al2O3
–12
–10
–8
–6
–4
–2
0
2
4
6
8
10
12
14
16
Component wt% Change from HW–39–4 Value

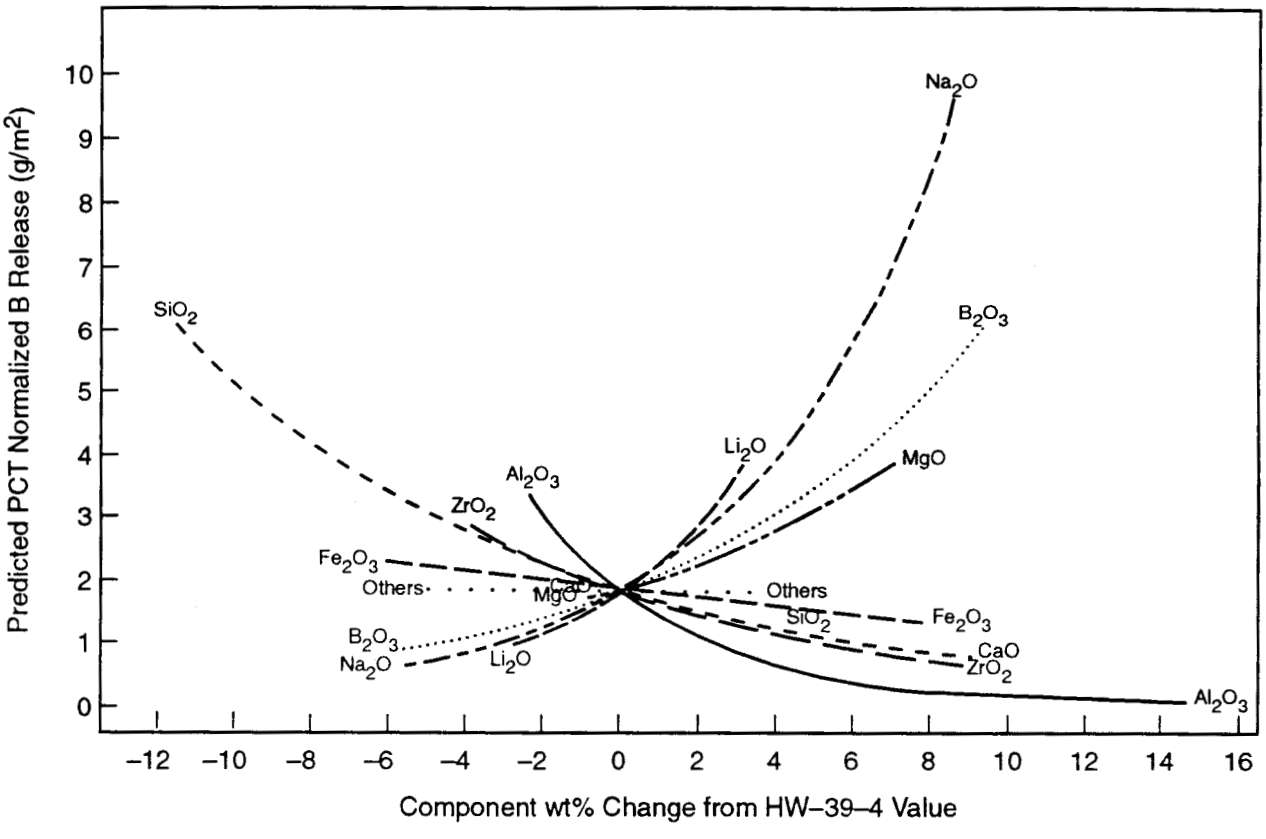
Predicted PCT Normalized B Release (g/m²)
Component wt% Change from HW–39–4 Value
Na2O
B2O3
MgO
Li2O
Al2O3
ZrO2
SiO2
Fe2O3
Others
CaO
MgO
SiO2
ZrO2
Li2O
Na2O
B2O3
Others
Fe2O3
CaO
Al2O3
0
1
2
3
4
5
6
7
8
9
10
–12
–10
–8
–6
–4
–2
0
2
4
6
8
10
12
14
16